Delayed postnatal brain development and ontogenesis of behavior and cognition in a mouse model of intellectual disability

Laurine Gonzalez, Catherine Sébrié, Serge Laroche, Cyrille Vaillend, Roseline Poirier

Neurobiology of Disease 183 (2023) 106163

Contents lists available at ScienceDirect

Neurobiology of Disease

journal homepage: www.elsevier.com/locate/ynbdi

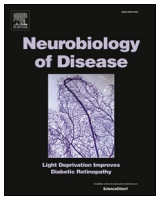

Delayed postnatal brain development and ontogenesis of behavior and cognition in a mouse model of intellectual disability

Laurine Gonzalez [a], Catherine Sébrié [b], Serge Laroche [a], Cyrille Vaillend [a], Roseline Poirier [a,*]

[a] Université Paris-Saclay, CNRS, Institut des Neurosciences Paris-Saclay, 91400 Saclay, France
[b] Université Paris-Saclay CNRS, CEA, Laboratoire d'Imagerie Biomédicale Multimodale (BioMaps), Service Hospitalier Frédéric Joliot, 91401 Orsay, France

ARTICLE INFO

Keywords:
Postnatal behavior
Intellectual disability
Neurodevelopmental disorders
Brain development
Cognitive development
Coffin-Lowry syndrome

ABSTRACT

Intellectual disability (ID) is a neurodevelopmental disorder associated with impaired cognitive and adaptive behaviors and represents a major medical issue. Although ID-patients develop behavioral problems and are diagnosed during childhood, most behavioral studies in rodent models have been conducted in adulthood, missing precocious phenotypes expressed during this critical time-window characterized by intense brain plasticity. Here, we selectively assessed postnatal ontogenesis of behavioral and cognitive processes, as well as postnatal brain development in the male *Rsk2*-knockout mouse model of the Coffin-Lowry syndrome, an X-linked disorder characterized by ID and neurological abnormalities. While *Rsk2*-knockout mice were born healthy, a longitudinal MRI study revealed a transient secondary microcephaly and a persistent reduction of hippocampal and cerebellar volumes. Specific behavioral parameters from postnatal day 4 (P4) unveiled delayed acquisition of sensory-motor functions and alterations of spontaneous and cognitive behaviors during adolescence, which together, represent hallmarks of neurodevelopmental disorders. Together, our results suggest for the first time that RSK2, an effector of the MAPK signaling pathways, plays a crucial role in brain and cognitive postnatal development. This study also provides new relevant measures to characterize postnatal cognitive development of mouse models of ID and to design early therapeutic approaches.

1. Introduction

Neurodevelopmental disorders (NDD) are characterized by altered cognitive and emotional development in childhood, which have a significant impact on academic achievements, social and domestic adaptive functioning. Among NDDs, intellectual disabilities (ID) have a prevalence of 1% of worldwide population and represent a major medical issue. According to The *Diagnostic and Statistical Manual of Mental Disorders* (DSM), ID is characterized by impairments in both intellectual functions and adaptive functioning arising during the postnatal period (DSM V, 2013). Deficits in intellectual functions are mainly assessed through standardized testing to evaluate the intellectual quotient (IQ). Adaptive functioning reflects the individual's ability to lead an independent life and comprises conceptual (language, reasoning, memory…), social (social judgment, communication…) and practical domains (personal care, organizing school or work tasks…), which are evaluated through standardized tests and interviews with patient's relatives and define the severity of ID (mild, moderate, or severe).

The genetic causes of ID are heterogeneous and represent 50% of reported cases (for a review, Marrus and Hall, 2017). They include chromosomal aberrations, copy number variants (duplications or deletions) and monogenic mutations. The last decades have witnessed remarkable acceleration in the discovery of novel ID-linked mutations that result from parental inheritance or dominant *de novo* mutations (McRae et al., 2017). IDs are often associated with alterations in brain development leading to morphological malformations that appear during the gestational and/or postnatal periods. Some macroscopic brain alterations such as macrocephaly, microcephaly or lissencephaly are detectable by medical imaging. However, certain mutations can also lead to molecular abnormalities without gross anatomical alterations,

Abbreviations: CLS, Coffin-Lowry syndrome; CZ, Clean zone; FOV, Field of view; ID, Intellectual disability; IQ, Intellectual quotient; ITI, Intertrial-intervals; KO, Knock-out; MAPK, Mitogen-activated protein kinase; MRI, Magnetic resonance imaging; MZ, Maternal zone; NDD, Neurodevelopmental disorder; P, Postnatal day; PRO, Procedural; *RPS6KA3*, Ribosomal Protein S6 Kinase A3; RSK2, Ribosome S6 Kinase 2; SPA, Spatial; TE, Echo time; TR, Repetition time; TSE, Turbo spin echo; WT, Wild type.

* Corresponding author.
E-mail address: roseline.poirier@universite-paris-saclay.fr (R. Poirier).

https://doi.org/10.1016/j.nbd.2023.106163
Received 29 March 2023; Received in revised form 17 May 2023; Accepted 18 May 2023
Available online 1 June 2023

but with an impact on several key cellular functions. Moreover, brain structures develop following a defined organization and during specific and precise time windows. A deviation of these key periods can affect the establishment and functioning of neuronal networks, leading to impaired brain development and emergence of cognitive deficits (Marco et al., 2011).

Among 1829 genes linked to ID (OMIM database, 2023), 192 are located on the X chromosome, including the *RPS6KA3* gene whose mutations are responsible for the Coffin-Lowry Syndrome (CLS). CLS is a rare genetic disorder characterized by moderate to severe ID: CLS-children display a low IQ associated with learning, memory, attention and concentration deficits, in addition to delayed or deficient acquisition of walking and language (Pereira et al., 2010). At birth, newborns appear normal after a pregnancy without difficulties. Then, physical and neurological abnormalities characteristic of CLS, such as growth retardation, hypertelorism, digit dysmorphism, thick lips and psychomotor deficits, become gradually apparent in the first years of life. In these patients, brain morphology has not been intensively studied, but some studies have reported cases of microcephaly, with some evidence that the hippocampal and cerebellar volumes may deviate from those of controls (Jacquot et al., 1998; Kesler et al., 2007). Male patients are generally more affected, while most female carriers have mild features. To date, there is no specific preventive or curative treatment for this syndrome, as only treatments targeting some clinical symptoms are used to improve patients' daily life. In spite of that, life span may be reduced in some CLS-patients, depending on the severity of comorbidities such as cardiac malformations, respiratory problems and epilepsy. Thus, it was reported that death between a mean range of 13–34 years occurs in 13,5% of males and 4,5% of females (Hunter, 2002; Coffin, 2003).

The *RPS6KA3* (or *RSK2*) gene is located at Xp22.2 and encodes the serine/threonine kinase RSK2 (Trivier et al., 1996). Among several CLS case reports and genetic studies, >260 different mutations resulting in a loss or non-functional protein have been reported (Database ClinVar 2023). To better understand how mutations in the *RSK2* gene contributes to cognitive impairments in CLS, we and others have previously studied a knock-out mouse lacking the *Rsk2* gene (*Rsk2*-KO; Yang et al., 2004). This mouse model displays delayed learning and memory deficits in spatial and working memory tasks, and an increased spontaneous activity related to emotional disturbances (Poirier et al., 2007; Fischer et al., 2017). The RSK2 protein has a crucial role in many brain physiological processes, such as synaptic plasticity and adult hippocampal neurogenesis, and its absence alters the Mitogen-activated protein kinase (MAPK) signaling pathway (Fischer et al., 2009; Mehmood et al., 2010; Schneider et al., 2011; Morice et al., 2013; Castillon et al., 2018). Although these studies have led to considerable progress in understanding *in vivo* functions of RSK2, they all addressed these functions at adulthood. During development, only two *in vitro* studies explored the role of RSK2 during embryogenesis and showed its implication in neuronal differentiation and neurite outgrowth (Dugani et al., 2010; Ammar et al., 2013). These specific roles of RSK2 have never been confirmed *in vivo*, but these data suggest that RSK2 deficiency could alter neurodevelopment, which may well cause the onset of ID-associated cognitive deficits. Although CLS is a NDD, the putative role of RSK2 in postnatal brain development and ontogenesis of behavior remains unexplored.

In the present study, we first identified secondary growth retardation and microcephaly in juvenile *Rsk2*-KO mice, supporting the hypothesis of major brain alterations during the postnatal period. The intense developmental brain plasticity that takes place at juvenile age warrants early behavioral assessment to further detail factors influencing the genesis of ID and to provide relevant outcome measures for preclinical studies aimed at evaluating the efficacy of treatments for these pediatric diseases. While behavioral protocols adapted for adult mice are fully developed (for review, Crawley, 1999), methods aimed at phenotyping newborn and juvenile mouse models of IDs are scarce. Therefore, we set up a behavioral test battery to evaluate the postnatal ontogenesis of reflexes induced by a variety of sensory stimuli, as well as early visuo-spatial cognitive performance, in juvenile mice from postnatal day 4 (P4) until P35. Our results highlight that postnatal exploration of mouse models of ID is a priority challenge for NDD research, as it may help to identify at the earliest, an optimal therapeutic window before establishment of persistent cognitive alterations.

2. Materials and methods

2.1. Animals

Rsk2-KO and wild-type (WT) littermate mice were generated and genotyped as previously described (Yang et al., 2004; Poirier et al., 2007). Pups from both genotypes were obtained by crossing C57BL/6 J males with heterozygous females generated in our mouse facility following >10 generations of backcrosses with the same parental strain. After a gestational period of 21 days, females gave birth to litters of normal size (2 to 8 pups). Newborn mice were kept in the mother's cage until weaning (at P21), under a 12 h light/dark cycle, constant room temperature (20–22 °C) and humidity (30–50%) with food and water *ad libitum*. Then, males from each litter were housed 3–5 per cage using polycarbonate shelters and cotton swap for nesting. All experimental procedures were conducted between 8:00 am and 6:00 pm, and in accordance with the guidelines of the European Communities Council Directive (2010/63/EU Council Directive Decree) and ethical committee (project n°APAFIS#11908–2017102410321573 v3). All efforts were made to reduce the number of mice and to minimize potential suffering. For some tests in which pups and juveniles could fall off the device, a 3 cm-thick mattress of cotton swap was placed below the apparatus to avoid painful falls.

For the present experiments, a total of 128 littermate male mice (72 WT and 56 *Rsk2*-KO) distributed across seven cohorts were used, with at least 3 different litters in each cohort (Fig. 1).

Postnatal brain development was assessed by MRI with a first cohort of mice (n = 5 per genotype), once a week over a period of 5 weeks beginning at the age of P14, and once at P56. Then, a second cohort (19 WT and 13 *Rsk2*-KO mice) was tested daily for reflexes acquisition, sensory modalities, and motor strength between P4 and P21. This same cohort was also evaluated in an open-field at P21 and in a cross-maze at P22. With a third cohort (6 WT and 7 *Rsk2*-KO mice), we tested performance in a one-day balance beam test followed by three consecutive days in a rotarod from P20 to P23. A fourth cohort (9 WT and 8 *Rsk2*-KO mice) was tested weekly in the two-odor choice test at P7, P14 and P21. To assess anxiety behavior, a fifth cohort (12 WT and 8 *Rsk2*-KO mice) was tested in the dark-light boxes test at P21. Finally, two protocols of water-maze were used to evaluate spatial and procedural memory with two different cohorts from P21 (cohort 6: 9 WT and 7 *Rsk2*-KO mice; cohort 7: 12 WT and 8 *Rsk2*-KO mice).

2.2. In vivo longitudinal MRI study

MRI was performed in a 7-Tesla preclinical magnet controlled by the Paravision software (Bruker Advance Horizontal 7-T Bruker, Inc., Billerica, MA) and equipped with a 22-mm-diameter "birdcage" antenna. Prior to MRI, each pup from cohort 1 was weighted and then anesthetized with isoflurane (1% with compressed air mix at 1 L/min). For MRI examination, mice were introduced in heated cradle adapted to animal size under anesthesia and kept warm throughout the entire experiment (around 9–10 min for the youngest mice and 25 min for adult mice). Due to the requirement for anesthesia, we were not able to perform MRI on mice before P14. In all cases, 5 to 10 min were required for MRI installation and adjustments (2D-FLASH: TR/TE: 100/30 ms; 1 average, 3 slices, 3 orthogonal directions; field of view (FOV): 40*40 mm; 30° flip angle; matrix 256*256; acquisition time 13 s). After MRI positioning and adjustments, different MRI sequences were realized: T1-weighted (T1w) 3D- Fast low angle shot magnetic resonance imaging

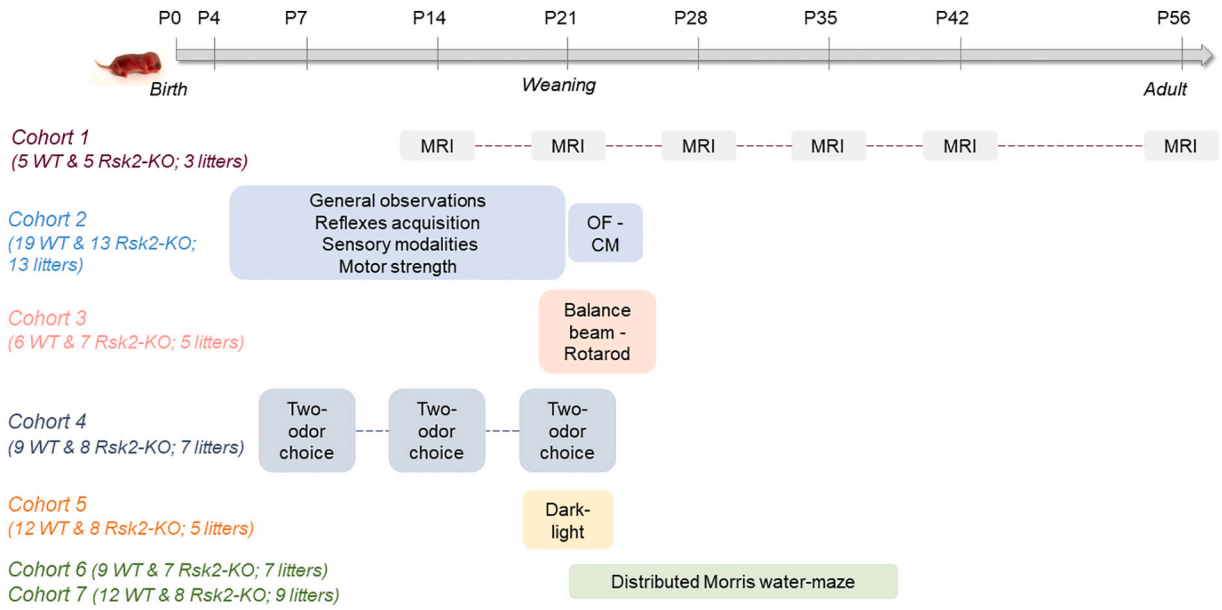

Fig. 1. Experimental design used in juvenile WT and *Rsk2*-KO mice. One cohort of mice ($n = 5$ per genotype) were assessed in MRI (Magnetic Resonance Imaging) once a week over a period of 5 weeks beginning at the age of P14, and once at P56. From P4, cohort 2 (19 WT and 13 *Rsk2*-KO mice) was daily weighted and tested in a battery of tests. From P21, this cohort was tested in open-field (OF) and cross-maze (CM) tests. A third cohort (6 WT and 7 *Rsk2*-KO mice) was tested at P20 in the balance beam test, followed the next three days by the rotarod test. A fourth cohort (9 WT and 8 *Rsk2*-KO mice) was tested at P7, P14, and P21 in a two-odor choice test. A fifth cohort (12 WT and 8 *Rsk2*-KO) was tested in the dark-light test at P21. Sixth and seventh cohorts (9/12 WT and 7/8 *Rsk2*-KO mice) were tested from P21 to P35/39 for spatial or procedural learning and memory in the water-maze.

(3D-FLASH-T1w: TR/TE: 55/8 ms, 1 average, 1 repetition; FOV: 20*20*12 mm, 20° flip angle, matrix 133*133*80, coronal orientation, acquisition time 10 min) and/or T2-weighted (T2w) 2D-Turbo spin echo (2D-TSE- > T2w: TR/TE: 4250/39 ms, 1 average, 8 repetitions, RARE factor: 8; FOV: 20*20 mm, matrix 256*256 size, axial orientation, 34 slices, 500 µm slice thickness, acquisition time 18 min). The first T1w sequence allowed to quickly measure brain volumes and larger intracerebral structures (necessary at P14 for an anesthesia of <10 min). The second T2w sequence had a longer duration allowing more precise measurements of each parameter. From P21, both MRI sequences were performed and did not detect any difference between measurements realized in the two sequences (different resolution and contrast). Resulting digital images were analyzed by marking brain areas in each slice using AMIRA® and ImageJ software. The volume of cerebellum, hippocampus, ventricles and cortex were analyzed and normalized to total brain volume.

2.3. Neurobehavioral development

From P4 to P21, longitudinal assessment of neurobehavioral development was performed by daily testing of littermate pups (cohort 2) by experimenters blind to the pup's genotype. Because early handling could perturb maternal behavior and induce cannibalism due to stress (Weber and Olsson, 2008), behavioral assessment only started from P4. To avoid separating pups from their mothers for too long periods during testing, pups were placed back in their mother's cage during intertrial-intervals (ITIs) and between tests. The recovery time between one observation and the following was approximately 5–10 min and no sign of stress was observed in individual pups or mothers. Each pup was weighted daily (±0.01 g), and then observed for 2 min to analyze *ambulation*. Four basic *ambulation* states were defined: crawling, in a transition state, starting to walk and walking (Feather-Schussler and Ferguson, 2016). Transition from crawling to walking was distinguished by observing hindpaws, head and tail raising, as described in Feather-Schussler and Ferguson (2016); Fig. 3.B).

Reflexes acquired during early postnatal development were assessed as previously described (Fox, 1965; Heyser, 2003; Feather-Schussler and Ferguson, 2016; Eltokhi et al., 2020). Each reflex was tested daily in cohort 2, and a score was given as follows: 0 = not present, 1 = weakly expressed, 2 = clearly present. Results were then expressed as the percent number of mice for which the response was seen at its maximal value (score = 2), or as the mean time needed to display the behavioral response.

Also described in human newborns, the *rooting reflex* is a primitive motor reflex, crucial for survival and growth because it allows newborns to find the source of food (Yoo and Mihaila, 2022). In juvenile mice, the experimenter used thumb and index fingers to perform a bilateral stimulation of the animal's face in three trials per day with 5 min ITIs. This stimulation induced a forward crawling behavior with the mouse pushing the head in a rooting manner (Fig. 3.C). The *grasping reflex* is a reflex observed at birth for forelimbs and at P12/14 for hindlimbs, consisting in grasping with fingers an object placed in front of the limbs. This reflex was tested in two successive trials per day and per limb (Fig. 3.D). The ability of pups to quickly upright themselves when placed upside down on their back is also an essential behavior for their survival. To assess this *surface righting reflex*, mouse pups were placed once on their back and held in this position for 5 s (Fig. 3.E). The latency to return to a prone position was recorded, with a cut-off latency of 30s. Likewise, when a mouse is facing a dangerous cliff, it is necessary for its survival to turn away to avoid falling. This reflex involves vestibular balance and is assessed using the *cliff aversion test.* This can be tested very early in juvenile mice, even at P4 when mice do not really move and do not open their eyes, because these are not the driving force to turn away. To test cliff aversion, pups were placed with their forepaws and nose over the edge of a 10 cm-high elevated box (Fig. 3.F). A lack of movement for 30s ended the trial. Finally, with the development of the vestibular system and motor coordination, the ability of pups to control their own body in the environment also develops during the postnatal period. The *negative geotaxis reflex* is tested by placing pups on an inclined plane facing down a 45° angle slope (Fig. 3.G). These last two tests were repeated in two consecutive trials with 5 min ITIs.

Regarding sensory modalities, tactile senses are established very early during postnatal development. To test the function of vibrissae, we used the *vibrissae placing response test.* When a mouse, suspended by its

tail, contacts with its vibrissae a solid object, it extends its head and forelimbs to grasp it (Fig. 3.H). This reflex appears around P4 and allows evaluating vibrissae sensibility and forelimb's and neck's muscle tones. The state of *eye opening* was checked every day from P10. An eye was considered open when a break in the eyelid was visible (Fig. 3.I). To assess hearing, we performed the *Preyer's reflex*, a method for distinguishing deaf animals (Jero et al., 2001). This technique involves an auditory stimulus consisting of a sharp metallic sound (around 110 dB) emitted in front of the pups (< 5 cm), leading to a reflexive reaction of the animal. This reaction was quantified and appears in the form of a contraction of the post-auricular muscles and a rapid startle movement of the whole body. Sometimes, at P19–21, a flight, escape-avoidance, behavior was observed instead of a startle response. Moreover, the contraction of the auricular muscle can also be tested with an *ear twitch* with a cotton swap (Fig. 3.K). This induces a slight movement response of the pup's ears and reflects development of head muscles and somatosensory function.

2.4. Motor behavior development

We used the *climbing (or grip strength) test* to assess limb muscle strength and motor coordination learning. This test adapted for juvenile mice could be used very early, even when pups were at a crawling state. From P4, pups were placed on a 24 × 37.5 cm grid with 0.5 cm spacing gaps between bars (Fig. 4.A) and a 45° tilt angle. The latency to fall was recorded (cut-off: 30s). This test was repeated daily in triplicates with 10 min ITIs. After 2 successful trials, we increased the tilt angle to 90°, then 135° and 180°. The mean fall latencies were plotted as a function of the tilt angle, at each age. At P21, all juveniles generally hold the grid bars for at least 30s from the upside-down grid (180°).

We also tested muscle strength in a *suspension test.* Suspension by hindlimbs was possible from P4, and by forelimbs from P10. For assessing hindlimb suspension, pups were placed face down with hindlimbs hung over the edge of one 50 mL canonical tube (Fig. 4.B). For forelimb suspension, pups were placed in traction, head up with the front legs on a wire bar. In both tests, two trials with a 10 min ITI were performed and the fall latencies were recorded.

From P20, we tested fine motor coordination and balance using a distinct cohort (cohort 3) submitted to the *balance beam test*. Mice had to walk across an elevated beam (length 80 cm, diameter 1 cm, Fig. 4.C) towards a black box containing nesting materials from their home cage. Juveniles were submitted to two consecutive trials with a 10 min ITI. The time to cross, and the number of foot flips and the falls were recorded. Twenty-four hours later, motor coordination and learning were evaluated using the *rotarod* task. Mice were placed on the rod for one training session during 3 consecutive days from P21 to P23 (Fig. 4.D). Each session comprised one trial in a stationary condition (60s), two trials in a constant speed condition (4 rpm, 60s), and two trials in an accelerating condition (1 to 40 rpm, 0–300 s) with 10 min ITIs. The time spent on the rod in each condition was recorded.

2.5. Spontaneous behaviors and cognition

For the following tests except the dark-light test, illumination was generated by indirect light (50 Lx in the two-odor choice, open-field and cross-maze tests, 380 Lx in the Morris water-maze) and all parameters were recorded by a video-tracking system (ANY-maze™ Stoelting, USA).

2.5.1. Two-odor choice test

Putative alterations in olfaction and development of exploratory behavior in juveniles during the postnatal period were assessed using a *two-odor choice test,* a classical choice test between maternal and neutral odors (Dierssen et al., 2002), using a distinct cohort (cohort 4). This test requires that juvenile mice move sufficiently; it was therefore performed at P7, P14 and P21. Briefly, the apparatus adapted from Bollen et al. (2012) was composed of two similar arms (20 cm long, V-shape, plastic-mesh floor) delimited by a neutral zone that can be closed by two Plexiglas doors. Each mesh arm was above two boxes that contained sawdust from the maternal cage (MZ, maternal zone) or clean sawdust (CZ, clean zone; Fig. 5.A) at positions randomized between tested mice. During testing, five consecutive choice tests of 1 min with 30s ITIs were performed, during which pups were placed individually in the neutral zone and could freely explore all zones after opening the door. To avoid odor diffusion, the experimenter used different gloves for manipulating odors and the V-maze was also cleaned between each trial with 70% alcohol. Travelled distance, latency to reach the maternal zone and distance travelled in the MZ were recorded.

2.5.2. Exploration of an open-field

At P21, juveniles from cohort 2 were observed during *exploration of an open-field.* The circular open-field arena (50 cm in diameter) had black sidewalls (35 cm high) and was covered with 2 mm of sawdust. Each juvenile mouse was placed near the wall and monitored during 20 min. Two zones were defined: a circular center zone and a peripheral zone (corridor of 5 cm in width). During this session, the distance travelled in the different zones was recorded to evaluate locomotion, exploration, anxiety (thigmotaxis). After 20 min, an object was placed in the center zone, which could freely be explored for 10 min, to address novelty-seeking behavior. The number of contacts exploring the object and travelled distance were recorded.

2.5.3. Dark-light box

We also tested anxiety with another group of mice (cohort 5) at P21 in a *dark-light choice test.* The apparatus consisted of a dark compartment (8 × 15 cm; <15 Lx) connected by an opened door to a brightly lit white compartment (30 × 15 cm), with 20 cm-high walls (Fig. 5.G). The illumination was provided by a light source placed at the end of the white compartment, opposite to the door to create an illumination gradient (30 Lx near the door to 1500 Lx close to the light). Each juvenile was placed in the dark compartment and could freely explore the apparatus during 10 min. Latencies, number of entries and travelled distance in the lit compartment were recorded.

2.5.4. Spontaneous alternation

At P22, 24 h after exploration in the open-field, spontaneous alternation was tested in a *cross-maze* with the second cohort. The apparatus consisted of a transparent maze with four arms (7.5 × 33 × 11 cm) radiating at 90° from a central area (7.5 × 7.5 cm). Juvenile mice were individually placed in the center of the maze and allowed to freely explore the four arms for 10 min. The number of visits and the temporal order of visits of each arm were recorded. Sequences of two, three or a maximum of four consecutive visits (Alt 2, 3, or 4) were analyzed, in order to quantify the number of sequences within which all visited arms were different. These alternation scores were normalized to the total number of visits and compared to chance levels, which were 75% for Alt2, 37.5% for Alt3 and 9.37% for Alt4. The chaining strategy (visiting 3 or 4 arms in clockwise or anti-clockwise order) was analyzed as indicators of stereotyped response patterns that may interfere with performance. To calculate this index, the sum of chaining visits was divided by the total number of visits minus 1 (the first visit can never be a chaining visit).

2.5.5. Spatial and procedural learning and memory

A water-maze was used to evaluate spatial and procedural navigation performance. The maze was a circular tank, 80 cm in diameter, filled with opaque water (addition of a white non-toxic paint). The water temperature was maintained at 22–24 °C. A non-visible circular platform (6 cm diameter) was placed 0.5 cm below the water surface. We used two different protocols with two different cohorts: a spatial version (SPA) in which different visible cues were placed on the room walls at <1 m distance (Fig. 6.A; cohort 6); and a procedural version (PRO) with no cue (Fig. 6.E; cohort 7). For both protocols, the day before training (at

P20), mice were submitted to one habituation session consisting of 3 consecutive trials, during which mice could swim freely during 60s to reach the immersed platform, placed in the center of the maze. If mice failed to find the platform, they were gently guided by experimenter's hand and remained on it for 30s before the next trial. The following days, for SPA version, juvenile mice were submitted to 2 sessions of 3 consecutive trials a day, separated by a 4 h interval. In this training phase, the platform was placed in the center of one specific quadrant, randomized between mice. For each trial, juvenile mice were introduced into the maze from different starting points and allowed to swim freely until they reached the platform (60s cut-off), on which they had to stay for 30s before the next trial. This training phase lasted for at least 8 days. Learning was stopped when a mouse reaches the learning criterion set at 80% success over the last two days (corresponding to a minimum of 10 successful trials out of 12 trials). A trial was considered as a success when mice reached the platform in <15 s, travelling <2 m. Otherwise, the learning phase was extended up to a maximum of 12 days. The day a mouse reached the criterion was noted. In the PRO version, mice were submitted from P21 to one session per day, consisting of 3 consecutive trials. Each mouse started all trials from one given starting point. The learning criterion was also set at 80% success, which here corresponded to a minimum of 5 successful trials out of 6 trials. In both versions (SPA and PRO), seven days after the end of training, a 60s probe test was performed consisting in a single trial during which the platform was removed. The video-tracking system recorded the distance travelled, swim speed and time spent in virtual areas of the maze: the four quadrants and a virtual peripheral zone set at 5 cm along the maze's wall, to quantify thigmotaxis. Memory retention was evaluated during the probe test by comparing the time spent in the target quadrant to chance level (25%), and analyzing the number of crossings over the platform position.

2.6. Statistical analyses

Data expressed as percent of mice are represented with the confidence interval and genotype differences analyzed using the Fisher's exact test in the R software. All other parameters are expressed as means ± SEM and successfully passed the normality test (Shapiro-Wilk test) and homogeneity of variance (Levene's test), and were therefore analyzed by factorial or repeated-measures ANOVAs or sample *t*-tests using the Jasp® software. When ANOVAs were significant, post-hoc Bonferonni comparison was used. Significance level was set at 0.05 for all analyses. To ensure the rigor and reproducibility of our data, we controlled the litter-to-litter variation (Lazic and Essioux, 2013; Jiménez and Zylka, 2021) by adding "litter" as an additional between-subject factor in our analyses of variance and by testing litter effect in Chi-square analyses. In a large majority of our observations, including the analysis of weight and brain volume in MRI experiments, we detected no litter effect (Supplementary table 1). In any case, rare detected litter effects concerned few isolated parameters, ages or tests, but any putative bias in these specific tests would not have modified our conclusions.

3. Results

3.1. The absence of RSK2 alters weight gain and delays postnatal brain development

As microcephaly has been detected in some CLS-patients (Jacquot et al., 1998; Kesler et al., 2007) and as we speculated a role of RSK2 in postnatal brain development, we performed a longitudinal MRI study in juvenile WT and *Rsk2*-KO mice from P14 to P42 and in adulthood (P56). Animals of this cohort were weighted once a week before imaging. A delayed weight gain was observed from P21 onwards (Fig. 2.A; strain effect: $F(1,8) = 13.22$, $p = 0.006$; age effect: $F(6,48) = 353.3$, $p <$

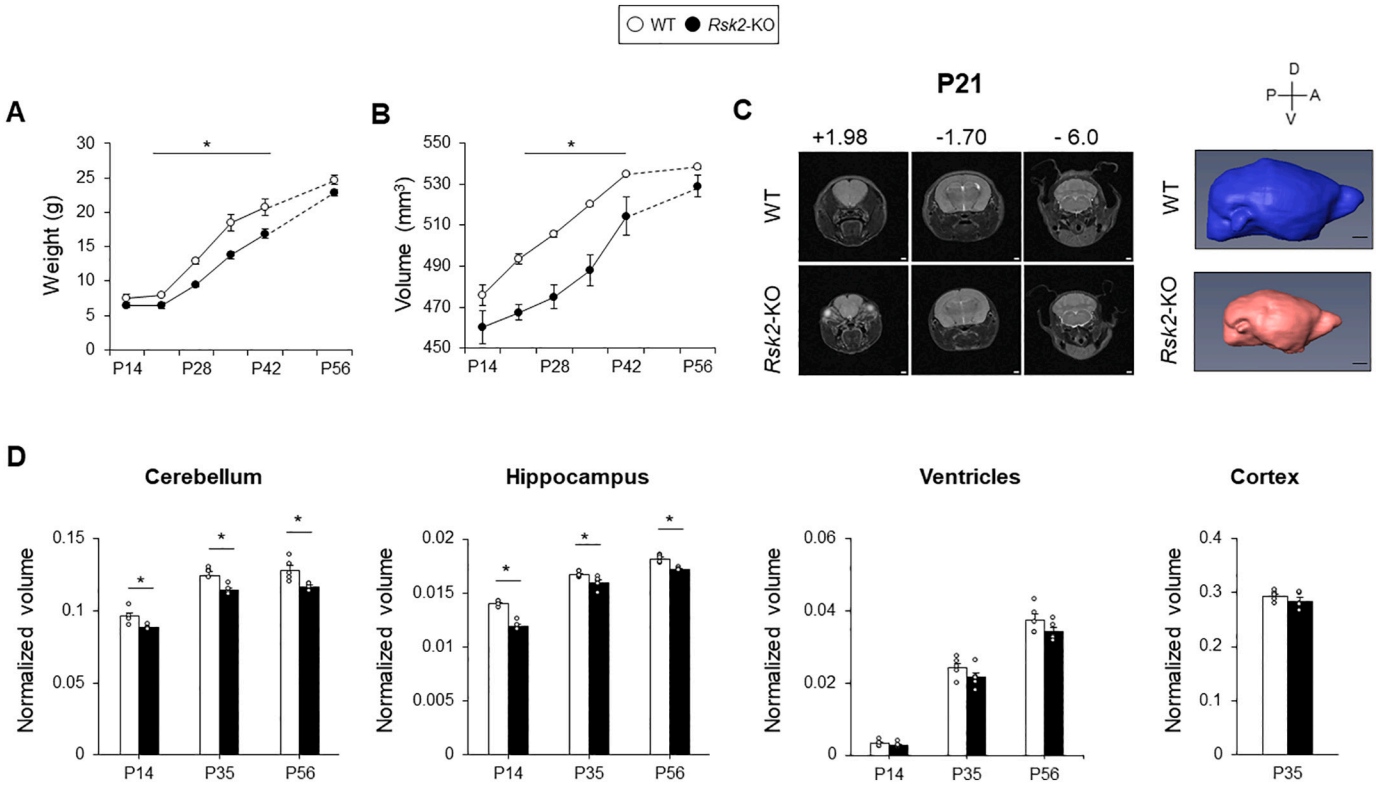

Fig. 2. Volumetric analyses of brain development and of different structures from a longitudinal MRI study. (A) Weight (g) as a function of postnatal day (P14 to P56) (B) Total brain volume measured by MRI (mm3) as a function of postnatal days (P14 to P56, $n = 5$ per genotype). (C) Examples of coronal sections and 3D representation of brains at P21 in a WT mouse (upper panel) and a *Rsk2*-KO mouse (lower panel; scale bar: 10 mm). (D) Volumes of cerebellum, hippocampus, ventricles and cortex normalized to total brain volume. * $p < 0.05$.

0.0001; interaction: F(6,48) = 3.494, $p = 0.006$), though the weight of *Rsk2*-KO mice became comparable to that of WT mice at P56 (Post-hoc Bonferroni comparison: P56: $p = 0.5182$). Thus, the slowdown in weight gain in the postnatal period is transient and recovers in adulthood. MRI analyses revealed a similar brain volume between genotypes at P14 (Fig. 2.B; F(1,9) = 2.966, $p = 0.1191$). From P21 to P42, however, there was a significant reduction of brain volume in *Rsk2*-KO mice compared to WT mice (Fig. 2.B, C; strain effect: F(1,8) = 12.413, $p = 0.0078$; age effect: F(4,32) = 137.615, $p < 0.0001$; interaction: F(4,32) = 4.132, $p = 0.0082$). Of note, the total brain volume recovered WT levels in adulthood (Fig. 2.B; Post-hoc Bonferroni comparison: P56: $p = 0.1046$), highlighting a delay in brain development in *Rsk2*-KO mice, which started after P14. Our analyses also revealed two distinct developmental phases: from P14 to P28, a slower increase in brain volume in *Rsk2*-KO mice was observed compared to WT mice. Then, from P28 to P56, the increase in brain volume accelerated, allowing recovery to WT brain volume level in adulthood. Finally, we also normalized brain volumes to body weights. We found that these ratios for *Rsk2*-KO mice were significantly different from those of WT mice (strain effect: F(1,8) = 13.179, $p = 0.007$; age effect: F(5,40) = 133.246, $p < 0.0001$; interaction: F(5,40) = 1.234, $p = 0.311$), indicating that the reduced brain volume in *Rsk2*-KO mice was not linked to their smaller body weights.

In rare reported clinical cases of CLS-patients with microcephaly, brain structures were found differentially impacted, showing reduced or dilated hippocampus, cerebellum and dilated ventricles (Kesler et al., 2007; Pereira et al., 2010). Here, we analyzed these different structures on MRI images in juvenile *Rsk2*-KO and WT mice at P14, P35 and P56. To take into account the smaller brain volume found in juvenile *Rsk2*-KO mice, measures from different structures were normalized to total brain volume. Normalized cerebellum volume from *Rsk2*-KO mice was found significantly smaller compared to that of WT mice from P14 to P56 (Fig. 2.D/Table 1; strain effect: F(1,8) = 13.514, $p = 0.0063$; age effect: F(2,16) = 363.558, $p < 0.0001$; interaction: F(2,16) = 0.994, $p = 0.391$). In the same way, normalized hippocampus volume from *Rsk2*-KO mice was significantly smaller compared to that of WT mice (Fig. 2.D/Table 1; strain effect: F(1,7) = 70.593, $p < 0.0001$; age effect: F(2,14) = 470.604, $p < 0.0001$; interaction: F(2,14) = 8.102, $p = 0.005$).

We also found these significant differences with the analysis of cerebellar and hippocampal volumes without the normalization to total brain volume (supplementary table 2). Thus, our data indicate that development of the hippocampus and cerebellum were particularly impacted in the absence of RSK2 during the postnatal period.

Regarding volumes of ventricles (all ventricles included) and cortex (analyzed at P35), significant reductions were observed in *Rsk2*-KO mice (supplementary table 2). But, once normalized to total brain volume, they were similar between genotypes regardless of the animal's age (Fig. 2.D; Ventricles: strain effect: F(1,8) = 4.876, $p = 0.06$; age effect: F(2,16) = 415.035, $p < 0.0001$; interaction: F(2,16) = 0.854, $p = 0.444$; Cortex: F(1,8) = 1.248, $p = 0.296$). Thus, these ventricles and cortex in *Rsk2*-KO mice appear reduced proportionally to the reduction of total brain volume.

3.2. *Rsk2-KO mice exhibit delayed neurobehavioral development*

As delayed brain development suggests alteration of functional development, we analyzed different neurobehavioral parameters at the earliest during the postnatal period. From birth, *Rsk2*-KO mice appeared healthy without overt developmental abnormalities. From P4 to P18, mice from both genotypes had comparable weights (Fig. 3.A). However, from P19, we confirmed the slowdown in weight gain previously observed in *Rsk2*-KO mice compared to WT mice (Figs. 2.A & 3.A; from P4 to P21: strain effect: F(1,30) = 1.4854, $p > 0.05$; day effect: F(17,510) = 1789.4, $p < 0.0001$; interaction: F(17,510) = 5.6863, $p < 0.0001$; Post-hoc Bonferroni comparison: P19: $p = 0.0335$; P20: $p = 0.0003$; P21: $p = 0.0001$). Thus, juvenile *Rsk2*-KO mice displayed a delayed gain in body weight that appeared during the 3rd postnatal week.

Regarding walking development state, at P7, 58% of WT mice were in the transition period (head and tail slightly raised), whereas >60% of *Rsk2*-KO mice were still crawling (Fig. 3.B; Fisher's exact test; strain effect: Crawling: $p = 0.0008$; Transition: $p = 0.007$). In a continuum, at P11, although almost all WT mice completely walked (95%), only 61% of *Rsk2*-KO mice were at this state, with 31% starting to walk and a small percentage (8%) still in transition (Fig. 3.B; Fisher's exact test; strain effect: Transition: $p = 0.006$; Start walking: $p = 3.54e\text{-}6$; Walking: $p = 8.34e\text{-}9$). However, even if the walking state of *Rsk2*-KO mice was delayed, they all ended up walking correctly at P13.

For the *rooting reflex*, only about 40% of the mice, whatever the genotype, presented this reflex at P4 (Fig. 3.C). From P6, all WT mice displayed the rooting reflex, whereas 2 more days were needed for all *Rsk2*-KO mice, highlighting a delayed acquisition. Then, as expected, this reflex disappeared with age, but still with a 2-day shift in *Rsk2*-KO mice (Fig. 3.C). For the *grasp reflex* (Fig. 3.D), all mice from both genotypes caught the object perfectly from P4 and kept this reflex stable over time (100% for each genotype at P4). The *surface righting reflex* was already expressed in few WT mice at P4, even if it took them more than 20s to upright themselves. In contrast, no *Rsk2*-KO mice could do it at this age within 30s (cut-off criterion). The latency to express this reflex rapidly improved over time in both genotypes but remained longer in *Rsk2*-KO mice compared to WT mice until P7 (Fig. 3.E; strain effect: F(1,30) = 21.077, $p < 0.0001$; age effect: F(9,270) = 100.078, $p < 0.0001$; interaction: F(9,270) = 3.679, $p = 0.0002$; Post-hoc Bonferroni comparison: P4: $p = 0.0065$; P5: $p < 0.0001$; P6: $p = 0.0007$; P7: $p = 0.0427$; P8: $p = 0.7337$; P9/P10/P11/P12/P13: $p > 0.9999$). *Rsk2*-KO mice finally reached the WT performance at P8.

Vestibular reflexes analyzed in *the cliff aversion* and *negative geotaxis* tests appeared from P5–6 in WT mice, but only at P8 in *Rsk2*-KO mice (Fig. 3.F-G), and a delay between genotypes persisted until P13–14. At P13, 100% of WT mice displayed these reflexes, whereas 100% of *Rsk2*-KO mice acquired this reflex only at P15 for cliff aversion and at P14 for negative geotaxis (Fig. 3.F-G; Khi-test interaction; cliff aversion: df = 9, $p = 0.0017$; negative geotaxis: df = 10, $p < 0.0001$). In summary, *Rsk2*-KO mice acquired all reflexes, but with a shift of several days compared to WT mice.

Tactile sensitivity evaluated using the *vibrissae-placing response* test revealed a similar increase with age in both genotypes, as shown by the increasing percentage of mice presenting the placing reflex over time (Fig. 3.H, Fisher's exact test, for each age $p > 0.09$), with 100% of mice showing optimal performance at P13. In contrast, eye opening was delayed by two days in all *Rsk2*-KO mice compared to WT mice (Fig. 3.I, Fisher's exact test, $p < 0.0001$). For hearing tested with the *Preyer's reflex*, half of the WT mice performed well at P16, whereas this percentage was reached at P17 for *Rsk2*-KO mice (Fig. 3.J; Fisher's exact test; P16: $p = 0.0006$; P17: $p = 0.02$). At P19, 100% of mice of both genotypes fully displayed the Preyer's reflex (Fig. 3.J), suggesting that *Rsk2*-KO mice did not present a major deficit in hearing. Somatosensory function tested with ear twitch was also slightly delayed in *Rsk2*-KO mice, with 100% of WT mice presenting this reflex from P13, whereas 100% of *Rsk2*-KO mice acquired this reflex at P14 only (Fig. 3.K.; Fisher's exact test, $p < 0.001$ for P11/12/13).

Table 1
Percent decrease in cerebellar and hippocampal normalized volumes of *Rsk2*-KO mice *vs.* WT mice, at three distinct ages (P14, P35, P56) and ANOVA results for genotype differences.

	Cerebellum	Hippocampus
P14	8.2%; F(1,8) = 11.415, $p = 0.0097$	14.7%; F(1,8) = 101.964, $p < 0.0001$
P35	8.3%; F(1,8) = 10.988, $p = 0.0106$	4.7%; F(1,8) = 7.522, $p = 0.0253$
P56	8.8%; F(1,8) = 10.308, $p = 0.0124$	5.2%; F(1,8) = 40.731, $p = 0.0002$

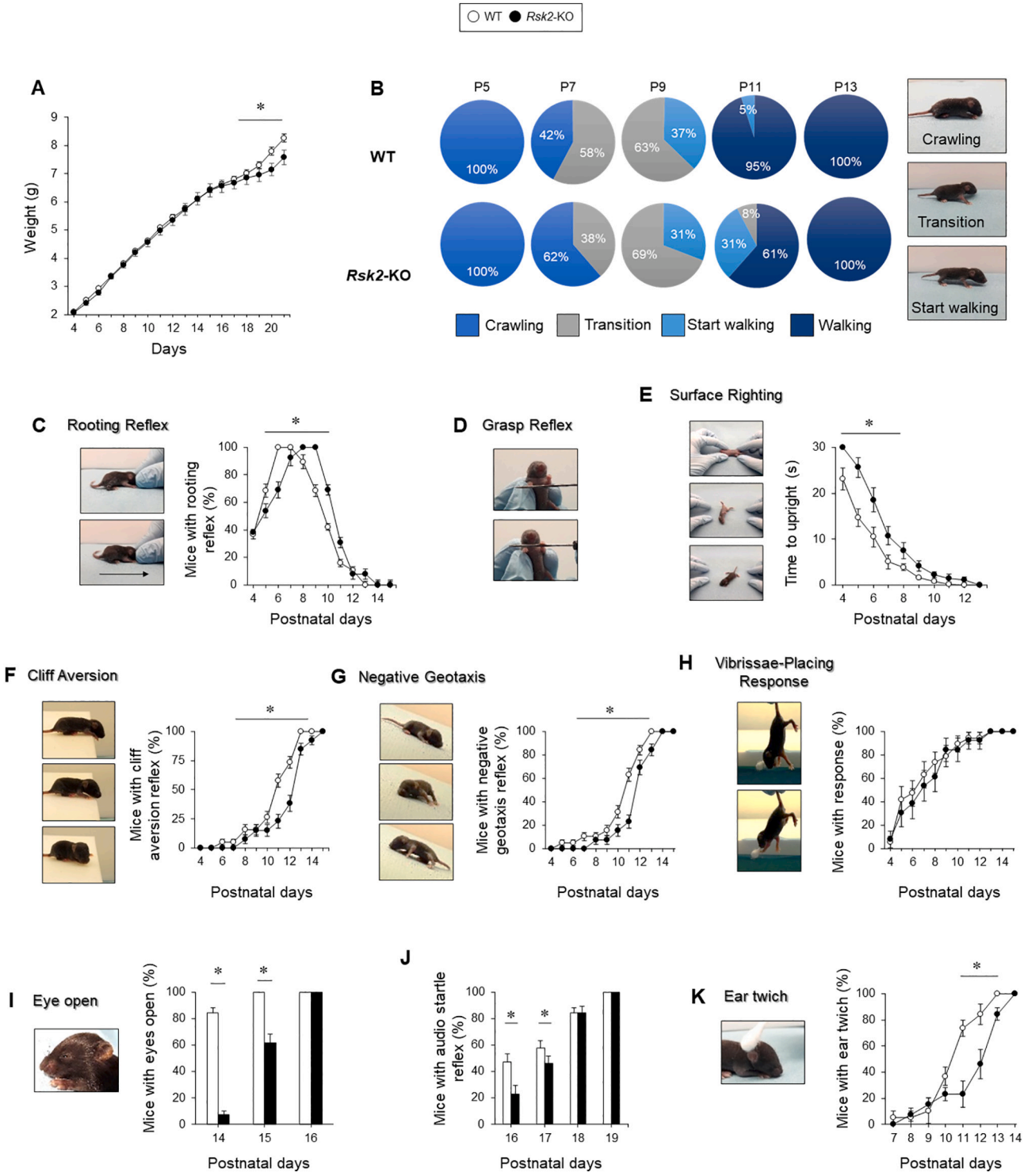

Fig. 3. General observations and acquisition of different reflexes and sensory modalities during the postnatal period. (A) Weight (± 0.01 g) of WT and *Rsk2*-KO mice from P4 to P21. (B) Percentage of WT (upper panels) and *Rsk2*-KO (bottom panels) mice at different ambulation states from P5 to P13. * $p < 0.05$. (C) Rooting reflex. Experimenter places two fingers on the face of the pups (up) and the animal crawls forwards pushing the head in a rooting manner (down). Graphs represent percentage of mice with rooting reflex from P4 to P15. (D) Grasping reflex to determine the plantar reflex. 100% of mice from both genotypes caught the object perfectly from P4. (E) Surface righting reflex. Latency to upright was recorded. (F-G) Cliff aversion and negative geotaxis. Plots represent percentage of mice presenting these reflexes. (H) Vibrissae-placing response test and percentage of mice showing the response. (I) Percentage of mice with eyes opened at P14, P15 and P16. (J) Percentage of mice with auditory startle during Preyer's reflex test. (K) Ear twitch test and percentage of mice with this reflex. * $p < 0.05$.

3.3. Juvenile Rsk2-KO mice display alteration in motor behavior development

Spontaneous motor behaviors were first assessed using the climbing test. As shown in Fig. 4.A, all mice from both genotypes succeeded when the grid was tilted at 45° with a slight improvement between P4 and P7 (Fig. 4.A; strain effect: $F(1,30) = 0.7597$, $p = 0.390$; age effect: $F(3,90) = 8.383$, $p < 0.0001$; interaction: $F(3,90) = 0.1958$, $p = 0.899$). From

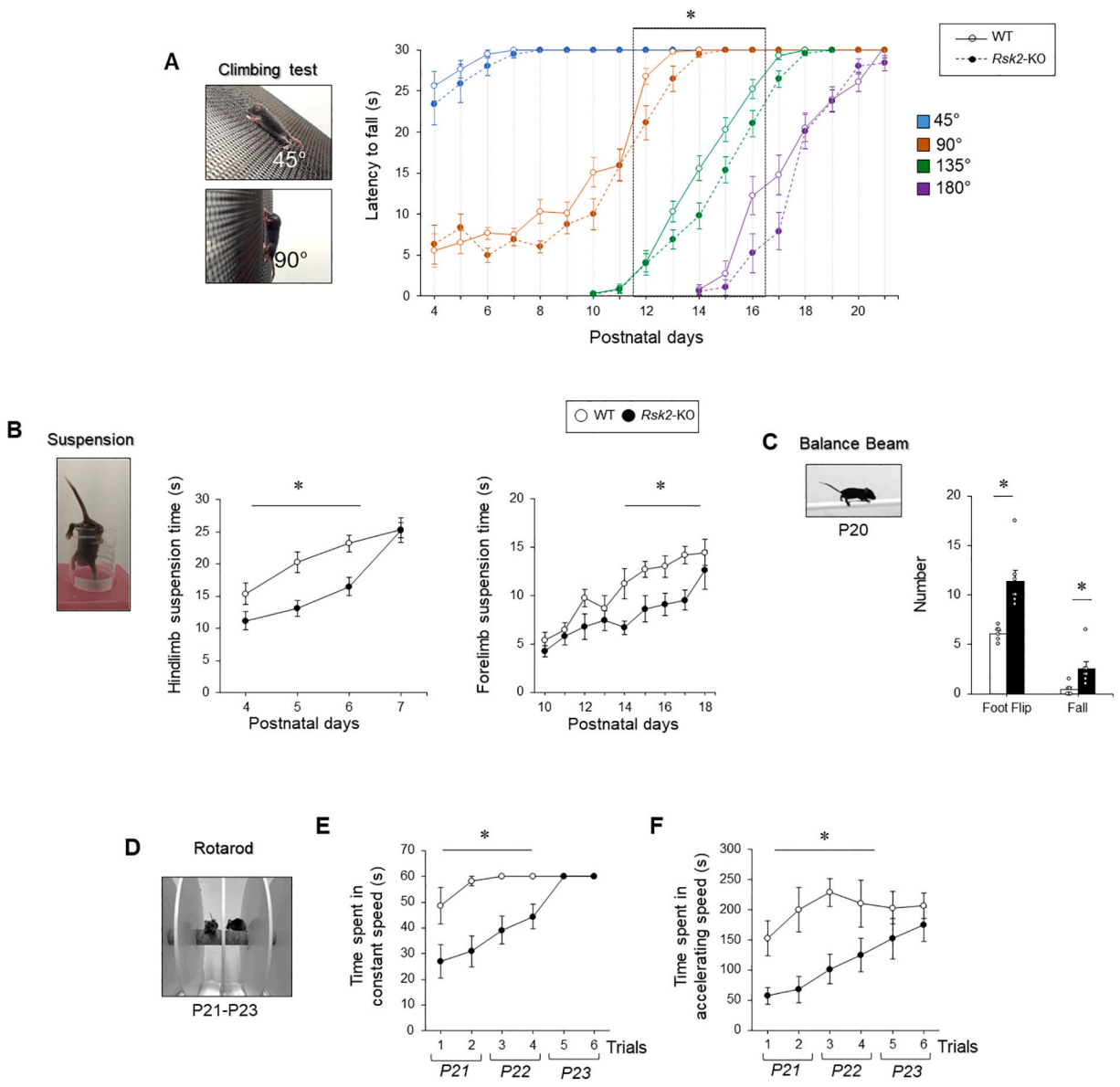

Fig. 4. Muscle strength development. (A) Climbing test. Latency to fall during each step of the exercise (tilt angle increasing) at each age for WT (full lines) and *Rsk2*-KO mice (dotted lines). (B) Suspension time (s) on canonical tube and wire bar. (C) Mean numbers of foot flips and falls during the balance beam test. (D) Rotarod task. (*E*-F) Time spent on the rod during trials in (E) constant speed and (F) accelerating speed (s) as a function of trial number, with two trials per day. * $p < 0.05$.

P12, whatever the grid tilt angle, *Rsk2*-KO mice did not last as long on the grid and had more difficulties in maintaining the same performance as that of WT mice (Fig. 4.A; 90° P12-P15: strain effect: $F(1,30) = 7.290$, $p = 0.0113$; age effect: $F(3,90) = 18.13$, $p < 0.0001$; interaction: $F(3,90) = 3.939$, $p = 0.0109$; 135° P10-P17: strain effect: $F(1,30) = 7.596$, $p = 0.0099$; age effect: $F(9,270) = 253.5$, $p < 0.0001$; interaction: $F(9,270) = 2.389$, $p = 0.0129$; 180° P14-P21: strain effect: $F(1,30) = 2.229$, $p = 0.1459$; age effect: $F(7,210) = 93.67$, $p < 0.0001$; interaction: $F(2,210) = 1.918$, $p = 0.0682$). Finally, *Rsk2*-KO mice displayed slight difficulties to succeed in the 180° test at P16-P17, but they reached the performance of WT mice for all exercises from P18. Together, these results suggest delayed motor strength development in *Rsk2*-KO mice. However, because our daily repeated test can engender a potential motor learning effect, we tested another group of naive mice (3 WT and 5 *Rsk2*-KO mice) at only P15 in 90° and 135° tests. For this additional naive group, *Rsk2*-KO mice fell after 12.91 ± 3 s whereas WT mice hold on the grid during 20.52 ± 2 s. These results are similar to those of the previous group, ruling out the possibility of delayed motor learning in *Rsk2*-KO mice in these conditions. Muscle weakness in *Rsk2*-KO mice has also been observed in the suspension test (Fig. 4.B), in which *Rsk2*-KO mice spent less time in suspension compared to WT mice, in particular during the hindlimb suspension test from P4 to P7 (strain effect: $F(1,30) = 10.052$, $p = 0.0035$; age effect: $F(3,90) = 29.238$, $p < 0.0001$; interaction: $F(3,90) = 2.9858$, $p = 0.0353$; Post-hoc Bonferroni comparison: P4: $p = 0.0471$; P5: $p = 0.0052$; P6: $p = 0.0096$; P7: $p > 0.05$), and during the forelimb suspension test from P14 (Fig. 4.B; strain effect: $F(1,30) = 6.944$, $p = 0.0132$; age effect: $F(8,240) = 5.286$, $p < 0.0001$; interaction: $F(8,240) = 0.92$, $p = 0.50$; Post-hoc Bonferroni comparison: P10-P13: $p > 0.05$; P14-P17: $p < 0.05$). As in the previous test, however, the time spent maintaining a grip onto the wire was comparable between genotypes at P18 (Fig. 4.B; $F(1,30) = 0.166$, $p = 0.68$).

Then, we tested balance and fine motor coordination in the *balance beam task* at P20. As shown in Fig. 4.C, *Rsk2*-KO mice did twice as much foot flips and falls than their WT littermates (Foot flips: $F(1,10) = 56.790$, $p < 0.0001$; Falls: $F(1,10) = 7.218$, $p = 0.023$) and, in consequence, they took longer to cross the bar ($F(1,10) = 1.764$, $p = 0.0214$). Nevertheless, we observed that *Rsk2*-KO mice crossed the bar in less than one minute on average. These results show that *Rsk2*-KO mice

display mild balance problems and slight defects in motor coordination at P20. In the rotarod task, mice were tested twice in three consecutive days from P21. Although we did not observe any difference between genotypes in the stationary trial (strain effect: $F(1,11) = 2.952$, $p = 0.114$; time effect: $F(2,22) = 2.952$, $p = 0.073$; interaction: $F(2,22) = 2.952$, $p = 0.073$), our results showed that *Rsk2*-KO mice spent significantly less time compared to WT mice when the rod was rotating at constant speed (Fig. 4.E; time effect: $F(5,50) = 10.058$, $p < 0.0001$; strain effect: $F(1,10) = 13.407$, $p = 0.004$; interaction: $F(5,50) = 4.105$, $p = 0.003$), as well as with accelerating rotation speed (Fig. 4.F; time effect: $F(5,50) = 3.898$, $p = 0.005$; strain effect: $F(1,10) = 7.249$, $p = 0.023$; interaction: $F(5,50) = 1.304$, $p = 0.278$). Of note, on the 3rd day of testing (P23), *Rsk2*-KO and WT mice had similar performance in both conditions reaching the optimal criterion on the rod at constant speed, and only falling from the rod at about 200 s in the accelerating speed condition. Together, these results show that juvenile *Rsk2*-KO mice have delayed muscle strength and motor coordination during the early phase of the postnatal period.

3.4. The absence of RSK2 modifies spontaneous behavior and leads to cognitive deficits in juvenile mice

In the *two odor-choice task*, all pups from both genotypes moved in the apparatus and travelled increasing distances with age (Fig. 5.B), thus revealing that *Rsk2*-KO mice did not present locomotor or motivational deficits in this task, although most of them were still crawling at P7. For both genotypes, the latency to reach the maternal zone (MZ) decreased with age. However, at P14 and P21, *Rsk2*-KO mice moved significantly faster to this zone (Fig. 5.C; strain effect: $F(1,15) = 7.033$, $p = 0.018$; age effect: $F(2,30) = 4.541$, $p = 0.019$; interaction: $F(2,30) = 0.799$, $p = 0.0459$). At P7, all pups from both genotypes moved at 80–100% over the maternal odor (Fig. 5.D; $F(1,15) = 0.362$, $p = 0.556$). However, we observed difference between genotypes with age (strain effect: $F(1,15) = 5.949$, $p = 0.028$; age effect:$F(2,30) = 14.148$, $p < 0.001$; interaction: $F(2,30) = 1.007$, $p = 0.377$; Post-hoc Bonferroni: P7-P14: $p = 0.168$; P14-P21: $p = 0.008$). In WT mice, the travelled distance in this zone significantly decreased from P7 to P21 ($F(2,16) = 4.976$, $p = 0.021$), in

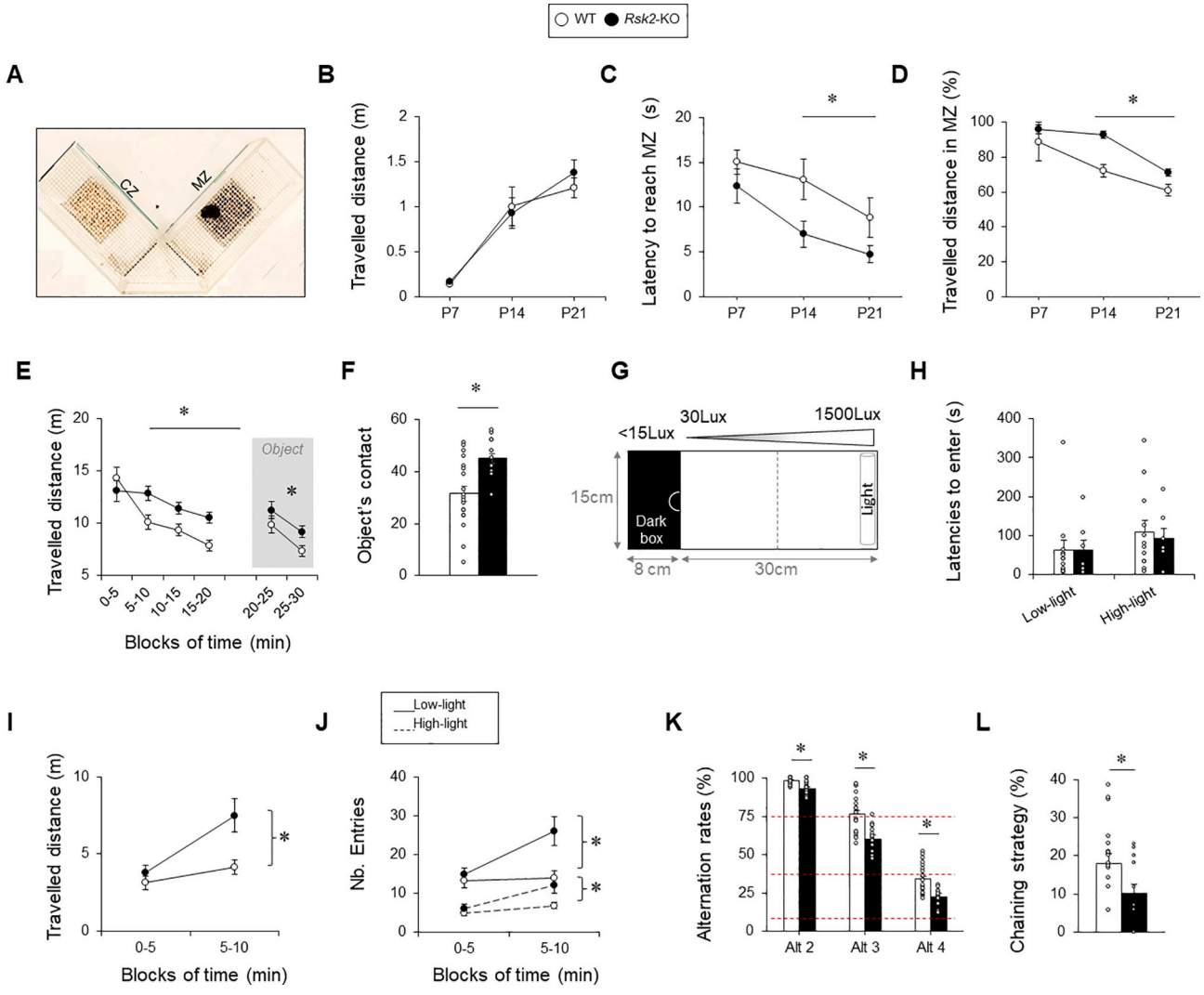

Fig. 5. Spontaneous behaviors of juvenile mice. (A) V-shaped apparatus used at P7, P14 and P21. MZ: maternal's odor zone, CZ: Clean zone. (B) Distance travelled (m), (C) latency to reach the MZ and (D) percentage of travelled distance in MZ at each age. (E) Distance travelled (m) in the open-field and (F) number of contacts with the object. (G) Schematic representation of the dark-light apparatus in top view tested in cohort 4 (12 WT and 8 *Rsk2*-KO mice). Dark and light compartments were connected by an open door. The light zone was separated in half by a virtual line (dotted line) to analyze behavior in the two parts with different light intensities. The light intensity gradient is schematized above. (H) Latencies to first exit and enter the most brightly lit zone. (I) Distance travelled. (J) Number of entries in different zones during 10 min. (K) Number of visits and temporal order of visits to individual arms in the cross-maze. All sequences of two (Alt 2), three (Alt 3) or four consecutive visits (Alt 4) were analyzed and the number of sequences of different arms visited was noted. Results were compared to chance levels (75% for Alt2, 37.5% for Alt3 and 9.37% for Alt4). (L) Chaining strategy in the cross-maze. * $p < 0.05$.

agreement with a crucial development stage occurring between P10 and P15 in rodents when juveniles begin to become independent of the nest and mother and develop exploratory behavior (Altman and Sudarshan, 1975; Lee and Williams, 1977; Wood et al., 2003). In contrast, the distance travelled by *Rsk2*-KO mice in the maternal zone significantly decreased only between P14 and P21 (P7-P21; $F(2,14) = 29.760$, $p < 0.0001$; Post-hoc Bonferroni: P7-P14: $p = 1.000$; P14-P21: $p < 0.0001$), suggesting a delay in their detachment from the mother.

In the open-field test at P20, *Rsk2*-KO mice showed normal locomotion activity and, as expected, the travelled distance decreased during the 20 min of the test due to progressive familiarization (Fig. 5.E). However, the distance travelled by *Rsk2*-KO mice was significantly higher compared to that of WT mice after the first 5 min (Fig. 5.E; strain effect: $F(1,30) = 1.167$, $p = 0.289$; distance effect: $F(3,90) = 71.927$, $p < 0.0001$; interaction: $F(3,90) = 5.739$, $p = 0.001$). When an object was introduced into the center area after 20 min, the latency to explore this object was similar for both genotypes ($F(1,30) = 0.316$, $p = 0.578$), but *Rsk2*-KO mice then travelled longer distances in the open-field (Fig. 5.E), spent more time and made more contacts with the object (Fig. 5.F; $F(1,32) = 19.535$, $p = 0.0001$). In these conditions, *Rsk2*-KO mice displayed hyperactivity when exposed to a novel environment and were more likely to explore the object than WT mice.

To assess anxiety-like behaviors, we first analyzed the percentage of distance travelled in the central zone of the open-field and these data showed comparable exploration of this zone between genotypes (Supplementary Fig. 1.A; strain effect: $F(1,30) = 1.889$, $p = 0.179$; time effect: $F(3,90) = 40.651$, $p < 0.0001$; interaction: $F(3,90) = 1.477$, $p = 0.226$). We also tried to use the elevated plus maze, but several young mice jumped out or tried to get down from the maze. We therefore tested anxiety-behavior in a dark-light choice test, with a gradient of light intensity (Fig. 5.G). In this test, latencies of the first entry in the lit zone, and latencies to reach the most brightly lit zone were similar between the two genotypes (Fig. 5.H; Low-light: $F(1,17) = 9.533e\text{-}4$, $p = 0.976$; High-light: $F(1,17) = 0.130$, $p = 0.723$). However, distances travelled in the different zones were longer in *Rsk2*-KO mice compared to WT mice after the 5th min (Fig. 5.I; strain effect: $F(1,17) = 7.268$, $p = 0.0153$; time effect: $F(1,17) = 29.81$, $p < 0.0001$; interaction: $F(1,17) = 9.611$, $p = 0.0065$). In the same way, between 5 and 10 min, *Rsk2*-KO mice made more entries into the lit zone (Fig. 5.J; strain effect: $F(1,17) = 6.560$, $p = 0.0202$; time effect: $F(1,17) = 12.29$, $p = 0.0027$; interaction: $F(1,17) = 9.419$, $p = 0.0069$), as well as into the brightly lit zone (Fig. 5.J; strain effect: $F(1,17) = 6.162$, $p = 0.0238$; time effect: $F(1,17) = 15.42$, $p = 0.0011$; interaction: $F(1,17) = 3.717$, $p = 0.0708$). Taken together, these results highlight that juvenile *Rsk2*-KO mice show no sign of anxiety but are slightly hyperactive after the first 5 min of exposure in these novel environments.

Finally, in the cross-maze assessing spontaneous alternation behavior, *Rsk2*-KO mice also travelled more distance after the 5th min (Supplementary Fig. 1.B; strain effect: $F(1,32) = 38.633$, $p < 0.0001$; duration effect: $F(1,32) = 23.775$, $p < 0.0001$; interaction: $F(1,32) = 7.220$, $p = 0.011$), but mice of both genotypes visited the same number of arms (Supplementary Fig. 1.C). Alternation rates were significantly different from chance for each alternation type (Fig. 5.K; One sample *t*-test, $p < 0.0001$ for Alt2, Alt3 and Alt4). However, *Rsk2*-KO mice alternated significantly less than WT mice (Fig. 5.K; Alt 2: $F(1,32) = 19.30$, $p < 0.0001$; Alt 3: $F(1,32) = 17.268$, $p = 0.0002$; Alt 4: $F(1,32) = 12.889$, $p = 0.0011$). Analysis of the chaining strategy evaluating the proportion of sequences of visits of 3 adjacent arms in the same direction, *i.e.* always turning clockwise or anticlockwise, showed that *Rsk2*-KO mice made significantly fewer visits to adjacent arms compared to WT mice (Fig. 5.L; $F(1,32) = 4.551$, $p = 0.041$). This indicates that *Rsk2*-KO mice did not preferentially used chaining strategies, which might have influenced the observed deficit in spontaneous alternation and could reflect stereotyped behaviors during the postnatal period.

Despite their young age, we were able to assess spatial learning and memory performance in *Rsk2*-KO mice from P21 using two different protocols in the Morris water-maze. In the standard spatial version (SPA protocol), juvenile mice could find the immersed platform using spatial cues available around the maze and started successive trials from different start points (Fig. 6.A). In the procedural version (PRO), visual cues were absent (Fig. 6.E) and juvenile mice had to learn one and the same trajectory, starting from the same start point at each trial. In both protocols, there was no difference in swim speed between genotypes during the training phase (SPA: D1-D8: strain effect: $F(1,14) = 3.717$, $p = 0.0744$; day effect: $F(7,98) = 3.274$, $p = 0.0036$; interaction: $F(7,98) = 0.3743$, $p = 0.9153$; PRO: D1-D8: strain effect: $F(1,18) = 14.652$, $p = 0.081$; day effect: $F(7,126) = 11.903$, $p < 0.0001$; interaction; $F(7,126) = 2.351$, $p = 0.027$), suggesting absence of gross motor alterations for swimming (Supplementary Fig. 2.A, B). In both tasks, juvenile *Rsk2*-KO mice took significantly more time and swam a longer distance to reach the platform during training (Time to reach the platform: SPA: Fig. 6.B; D1-D8: strain effect: $F(1,14) = 35.06$, $p < 0.0001$; day effect: $F(7,98) = 32.77$, $p < 0.0001$; interaction: $F(7,98) = 2.254$, $p = 0.0361$; PRO: Fig. 6.F; D1-D8: strain effect: $F(1,18) = 22.864$, $p = 0.0001$; day effect: $F(7,126) = 26.487$, $p < 0.0001$; interaction: $F(7,126) = 1.988$, $p = 0.042$; Travelled distance: SPA: Fig. 6.C; D1-D8: strain effect: $F(1,14) = 28.36$, $p = 0.0001$; day effect: $F(7,98) = 25.15$, $p < 0.0001$; interaction: $F(7,98) = 2.662$, $p = 0.0145$; PRO: Fig. 6.G; D1-D8: strain effect: $F(1,18) = 14.92$, $p = 0.0011$; day effect: $F(7,126) = 7.463$, $p < 0.0001$; interaction: $F(7,126) = 4.668$, $p < 0.0001$). Analysis of thigmotaxis during training showed that *Rsk2*-KO mice spent more time in the peripheral zone compared to WT mice (SPA: Fig. 6.D; D1-D8: strain effect: $F(1,14) = 12.73$, $p = 0.0031$; day effect: $F(7,98) = 33,41$, $p < 0.0001$; interaction: $F(7,98) = 0.5908$, $p = 0.7620$; PRO: Fig. 6.H; D1-D8; strain effect: $F(1,18) = 18.262$, $p < 0.0001$; day effect: $F(7,126) = 27.946$, $p < 0.0001$; interaction: $F(7,126) = 2.020$, $p = 0.057$). Thus, in this specific task, juvenile *Rsk2*-KO mice could display slight signs of anxiety, although anxiety has not been observed in other conditions (open-field; dark-light tasks). Finally, in both versions, all *Rsk2*-KO mice reached the learning criterion later than WT mice (11–12 days for *Rsk2*-KO mice against 8–9 for WT mice; SPA: $F(1,14) = 301.881$, $p < 0.0001$; PRO: $F(1,18) = 10.890$, $p = 0.004$). In each version, two *Rsk2*-KO mice never reached the set criterion after 12 days of training and were therefore removed from the analysis.

To assess long-term memory restitution, a probe test was realized seven days after the end of training. In the SPA version, WT mice spent significantly more time in the target quadrant (Fig. 6.I; Student *t*-test, $t(8) = 5.133$, $p = 0.0009$), whereas *Rsk2*-KO mice performance did not differ from chance level (25%), with equivalent time spent in each quadrant (Student *t*-test, $t(6) = 1.047$, $p = 0.3354$). During the retention test, *Rsk2*-KO mice did not show more thigmotaxis than WT mice (Supplementary Fig. 2.C). These results unveiled a major deficit in spatial long-term memory in *Rsk2*-KO mice. Moreover, the number of crossings was significantly different between WT and *Rsk2*-KO mice (Fig. 6.J; $F(1,14) = 10.815$, $p = 0.005$). Of note, in the PRO version, all mice from both genotypes spent more time in the target quadrant (Fig. 6.K, *t-test vs chance*, WT: $t(11) = 4.150$, $p = 0.0008$; *Rsk2*-KO: $t(7) = 2.996$, $p = 0.01$), and showed similar number of crossings in the target quadrant (Fig. 6.L; $F(1,18) = 1.245$, $p = 0.279$), suggesting an absence of memory deficit in the procedural version. In all, in agreement with Chapillon et al. (1995), we confirm that spatial and procedural learning can be assessed early in juvenile mouse models and we show that long-term memory retention can be evaluated seven days after learning. We further show that the absence of RSK2 is associated with delayed spatial and procedural learning, impaired spatial long-term memory, but normal procedural memory consolidation and retention.

4. Discussion

In the present study, we report for the first time, in parallel with a slowdown of weight gain, a secondary microcephaly appearing from the second postnatal week in the juvenile *Rsk2*-KO mouse model of the

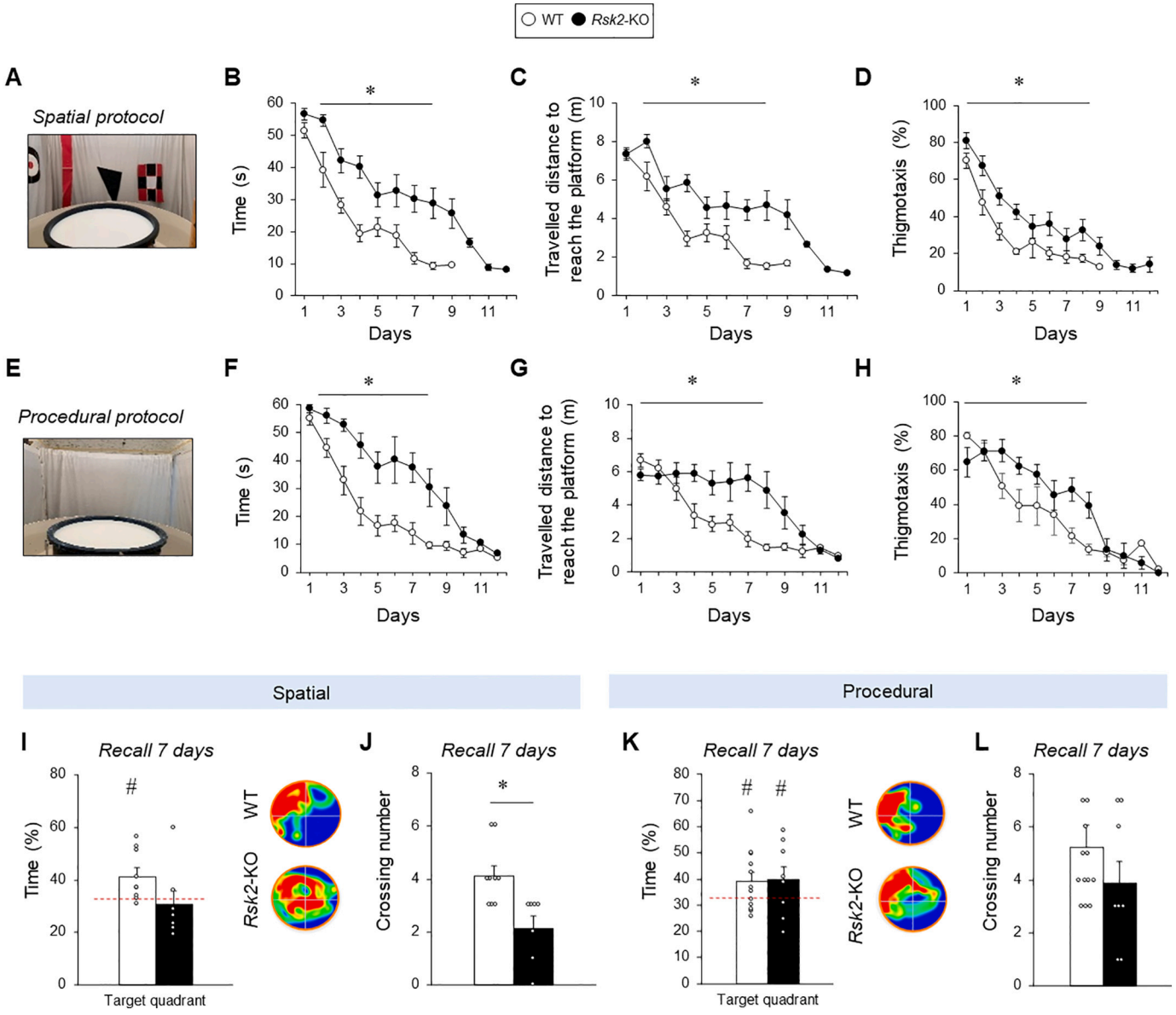

Fig. 6. Spatial and procedural learning and memory in WT and *Rsk2*-KO mice from P21 to P39. (A) Water-maze used in the spatial protocol (SPA) with cues on walls. (B—D) Spatial learning phase: (B) time and (C) distance to reach the platform, (D) time spent in periphery (thigmotaxis). (E) Water-maze used in the procedural protocol (PRO) with no cue on walls. (F—H) Procedural learning phase: (F) time and (G) distance to reach the platform, (H) time spent in periphery (thigmotaxis). (I-L) Long-term retention in both protocols. Time in target quadrant in (I) spatial and (K) procedural protocols is expressed as a percentage of total time. Red dotted lines represent chance level (25%). Examples of tracking for WT (up) and *Rsk2*-KO mice (down) during the retention test. Red color represents a longer time in the zone. Mean number of crossings in (J) spatial and (L) procedural protocols. * $p < 0.05$.

Coffin-Lowry syndrome, which recovers in adulthood, except for a lasting impact up to adulthood on hippocampal and cerebellar development. These results reinforced the idea of studying the ontogeny of behaviors and in particular those related to cerebellum and hippocampus functions. Moreover, our extended phenotypic characterization of a juvenile mouse model of ID highlights the potential of postnatal behavioral screening to detect early hallmarks of neurological and cognitive deficits in mouse models of NDD associated with ID. Thus, our behavioral test battery demonstrates for the first time that juvenile *Rsk2*-KO mice display a significant delay in achieving key reflexes and sensorimotor milestones, before the appearance of microcephaly, as well as alterations in spontaneous behaviors and cognitive processes, results that are consistent with the behavioral and cognitive deficits found as typical hallmarks of ID.

At birth, CLS-patients display growth parameters within the normal range, but clinical case reports indicate that delays in growth and weight appear around the age of 2–3 years (Manouvrier-Hanu et al., 1999; Pereira et al., 2010; Miyata et al., 2018; Lv et al., 2019). Here, tracking for the first time postnatal development of the CLS mouse model, we show that although the weight of *Rsk2*-KO pups was similar to that of WT mice during the two first postnatal weeks, their weight gain slows down during the third week. Often described in adults, the smaller body weights of CLS mouse models remain relatively modest (Dufresne et al., 2001; El-haschimi et al., 2003; Yang et al., 2004; Poirier et al., 2007; Fischer et al., 2017) and have notably been attributed to the involvement of RSK2 in osteoblast differentiation (Yang et al., 2004), skeletal muscle differentiation (Cho et al., 2007) and regulation of adipose tissue (El-haschimi et al., 2003). From P20-P21, mice typically show an intensive growth of muscle fibers volume and a transient period of adipose tissue remodeling responsible for increased body fat (Gattazzo

et al., 2020; Bruder and Fromme, 2022). Here, although this was not specifically examined, we speculate that the absence of RSK2 leads to a slowing-down in skeletal/muscular and fat mass gain that could have an impact on the development of motor functions. Associated with these musculoskeletal abnormalities, we first observed a delay in walking acquisition in agreement with abnormalities described in some young CLS-patients (Herrera-Soto et al., 2007; Pereira et al., 2010). This delay in the development of motor abilities could well be due to alterations in muscle strength, posture and motor coordination in *Rsk2*-KO mice during the first postnatal days. Muscle weakness in juvenile *Rsk2*-KO mice is also supported by the meager performance of *Rsk2*-KO mice in climbing and suspension tests between P13 and P17, when performance of WT mice rapidly improves and/or when the exercise difficulty intensifies. Interestingly, we found that these defaults recover before weaning in accordance with the absence of deficits in muscle strength or coordination previously reported in adult *Rsk2*-KO mice (Poirier et al., 2007), suggesting a delayed development rather than a major dysfunction.

Exploring several developmental reflexes, we also show that juvenile *Rsk2*-KO have a general delay in neurobehavioral development during this early postnatal period, thus revealing defaults in the maturation of specific functional domains. In addition to a delay in gait acquisition, some of the earliest reflexes were also delayed by few days, such as surface righting, cliff aversion and negative geotaxis reflexes. All these reflexes require trunk control and dynamic postural adjustments, and depend on the integrity of sensorimotor and proprioceptive functions, which also involve the vestibular system and cerebellar functions (per review Lopez, 2015; Schmahmann, 2019). At birth, the vestibular system and cerebellum are quite well developed, but continue to mature markedly until P32 and P35 respectively, and vestibular cells connect to the cerebellum and spinal cord during the first two postnatal weeks (Hibi and Shimizu, 2012; Jamon, 2014; Haldipur and Millen, 2019). Hence, the difficulties displayed by young *Rsk2*-KO mice in walking and in early reflexes suggest disturbances of vestibular system development and/or delayed cerebellar maturation. This hypothesis is supported by our MRI imaging results showing that cerebellar volume is reduced in *Rsk2*-KO mice from P14 and suggests alterations in cellular/molecular processes occurring during their postnatal period. At P21/22, their low performance in the balance beam and rotarod tasks also reinforces this interpretation. Of note, however, these defaults are transient and the progressive increase in performance over time indicates that motor learning in *Rsk2*-KO does not seem fundamentally impacted. In CLS-patients, musculoskeletal abnormalities have been reported (Herrera-Soto et al., 2007; Pereira et al., 2010), but the integrity of vestibular functions has never been extensively studied. Balance problems were previously described in clinical cases and one study in a one-year-old patient reported labyrinthine anomalies (Higashi and Matsuki, 1994). Moreover, even if we lack detailed clinical case studies, one study reported alterations of cerebellar volume (Kesler et al., 2007). Unfortunately, except for this publication, no study specifically focused on the cerebellum in CLS-patients or in the CLS mouse model, and it may be of interest to investigate the cellular processes and cerebellar maturation underlying postnatal cerebellar development in this mouse model in future studies.

Regarding other sensory modalities, we found that reflexes such as the grasp reflex observed from P4 and the placing response requiring tactile stimulations were not affected. Although we did not perform any specific test for olfactory or visual abilities, our observations of spontaneous behaviors in several conditions do not suggest gross anomalies. For example, in the two-odor choice task, *Rsk2*-KO mice quickly reached the maternal zone based on olfactory cues. Moreover, although eye opening in *Rsk2*-KO pups was delayed, their normal performance in the visual placing response, object exploration or in other behavioral tasks, indicate no major alterations of vision after a few weeks of development. Regarding the auditory system, we observed a delay in achieving the Preyer's response in *Rsk2*-KO mice but, by P18, all mice acquired this acoustic reflex. Taken together, our results show that the absence of RSK2 delays sensory development, which may have important implications because sensory inputs during a precise critical period are needed for the normal development of associated brain regions (Lo et al., 2017). Thus, we anticipate that delays in the development of certain sensory modalities can alter the normal establishment of neuronal networks in the CLS mouse model.

We also found behavioral and cognitive alterations in young *Rsk2*-KO mice, that were already reported in adult *Rsk*2-KO mice (Poirier et al., 2007; Fischer et al., 2017), but with some differences. Adult *Rsk2*-KO mice are more active in some specific situations, but not when they are placed in an open-field or in an IntelliCage® (Poirier et al., 2007; Fischer et al., 2017). Adult *Rsk2*-KO mice also show certain stereotyped behaviors, a slight disinhibition in exploratory activity, and a trend to be hyper-reactive to environmental stimuli in certain situations (Poirier et al., 2007). In young *Rsk2*-KO mice, these features seem to intensify with, for instance, impaired spontaneous alternation reflecting stereotypies, and hyperactivity when mice are placed in an unknown environment (open-field, cross-maze, dark-light choice apparatus). These data suggest important difficulties in adapting to new situations, which corresponds to certain characteristics of ID.

Finally, we found that adolescent *Rsk2*-KO mice (after weaning) display both procedural and spatial learning deficits and a long-term spatial memory deficit, two forms of learning and memory that are substantiated during the juvenile period (for reviews, Wood et al., 2003; Hubert et al., 2007). Of note, for both forms of learning, extended training allowed the majority of juvenile *Rsk2*-KO mice to reach the performance level of WT mice, highlighting a delay in learning. Then, in the procedural, egocentric version of the task, in which mice can learn by using one and the same stable navigation trajectory, they showed unaltered recall performance during the retention test, suggesting that, once acquired, long-term procedural memory is efficient. In contrast, despite reaching the same performance as that of WT mice after extended training, long-term spatial memory 7 days after acquisition requiring an allocentric strategy was deficient in juvenile *Rsk2*-KO mice, suggesting deficient consolidation and/or long-term spatial retrieval. This is a similar spatial memory deficit as that we previously found at the adult age (Poirier et al., 2007; Castillon et al., 2018). These results strongly suggest alterations of hippocampal and/or cerebellar function, which is supported by our MRI results showing a significant reduction in hippocampal and cerebellar volumes from P14 onwards in *Rsk2*-KO mice, in agreement with a report showing reduced hippocampus and cerebellum in CLS-patients (Kesler et al., 2007). During the postnatal period, these structures display significant growth with a large number of ongoing cellular processes such as cell proliferation, differentiation, and expansion of connectivity within neuronal networks (Sudarov and Joyner, 2007; Khalaf-Nazzal and Francis, 2013; Hirano, 2018). At birth, the brain of newborn mice only reaches 20% of its final volume, and then develops intensely during the first 3 weeks of life (Chuang et al., 2011; Semple et al., 2013). Brain development during this period is associated with neurogenesis, gliogenesis and dendritic growth that peaks around P7-P10 (Rice and Barone, 2000; Semple et al., 2013), while dendritic growth, apoptosis and myelination continue during the next weeks of postnatal development to allow progressive brain growth. The secondary microcephaly found in *Rsk2*-KO mice from P14 suggests that at least some of these neurodevelopmental processes are impacted. One possibility is that the absence of RSK2 could delay dendritic and axonal growth, an hypothesis supported by *in vitro* studies of embryonic cortical neurons demonstrating a role for the RSK2 protein in neuronal differentiation and neuritic outgrowth (Dugani et al., 2010; Ammar et al., 2013), as well as in axonal growth (Fischer et al., 2009). A potential underlying mechanisms may involve dysregulation of MAPK signaling in absence of RSK2, as reported in adult mice (Schneider et al., 2011), during the postnatal period since activation of ERK1/2 gradually increases during the postnatal period (Costa et al., 2016) and is known to be involved in brain developmental processes (Sun et al., 2016; Albert-

gasco et al., 2020). Finally, because we previously reported deficient adult hippocampal neurogenesis and hippocampal synaptic plasticity in adult *Rsk2*-KO mice (Morice et al., 2013; Castillon et al., 2018), these forms of plasticity could already be deficient during the postnatal period and thus be, at least in part, responsible for the impaired cognitive functions. Additionally, Mehmood et al., 2010 have reported an increased GluR2 expression in adult hippocampal *Rsk2*-KO mice, leading to AMPA neurotransmission deficit, a mechanisms that would be interesting to study during the postnatal period because synaptic AMPA subunits composition changes during development (Henley and Wilkinson, 2016). Future directions will involve determining the relevant cellular/molecular mechanisms that may be responsible for the observed alterations in brain development and cognitive deficits.

To conclude, beyond the interest in providing novel information relevant to CLS, the present results underscore the relevance of postnatal screening for NDDs. For several decades, numerous mouse models of ID have been generated that are of wide interest to investigate gene-brain-behavior relationships (Vissers et al., 2015). If genes involved in NDD affect the formation of neuronal circuits and their plasticity during postnatal development, specific pharmacological and behavioral interventions could be considered to prevent or compensate the genesis of sensory, motor, behavioral and cognitive deficits at the earliest. However, only few studies have examined ontogenesis of behavior and brain development during the postnatal period in mouse models of ID. For example, some authors reported developmental delay in acquisition of reflexes, sensory and motors milestones, as wells as abnormal spontaneous behaviors and cognitive impairments in different models of Down Syndrome (Holtzman et al., 1996; Altafaj et al., 2001; Toso et al., 2008; Olmos-Serrano et al., 2016; Llambrich et al., 2022), Rett syndrome (Picker et al., 2006; Santos et al., 2007) and Fragile X syndrome (for a review, Razak et al., 2020). Only few studies have examined brain volume in these animal models of ID, showing, as found here, alterations in brain volume during the postnatal period, with a definite impact on the hippocampus and cerebellum (Shi et al., 2012, 2020; Llambrich et al., 2022). Our present results in the mouse model of CLS highlight similar abnormalities and suggest that RSK2 protein plays a key role in postnatal brain and cognitive development. The *Rsk2*-KO model may therefore be particularly useful to understand the genesis of ID-associated cognitive deficits, such as in RASopathies caused by genetic mutations affecting proteins of the RAS/MAPK pathway that activates RSK2 (for review, Rauen, 2013). Finally, clinical signs appear during the developmental period in patients with NDD. Because brain development involves comparable mechanisms in humans and mice, and similar pathological alterations were described in both species (for review, Semple et al., 2013), postnatal mouse studies have a strong translational value. The evaluation of postnatal ontogenesis of behavior in rodents therefore appears to be an important step towards a better understanding of the physiopathology of pediatric diseases and to open the way for new and precocious therapeutic strategies.

Author contributions

L.G. and R.P. designed and performed the experiments. L.G. and C.S. carried out MRI study. L.G., R.P., C.V. and S.L wrote the manuscript. All authors have read and agreed to the published version of the manuscript.

Declaration of Competing Interest

The authors declare no competing interests.

Data availability

Data will be made available on request.

Acknowledgments

This work was supported by the Centre National de la Recherche Scientifique (CNRS, France); University Paris-Saclay (France); the Jerome Lejeune Foundation (Grant #1840 to RP); Xtraordinaire association (to RP and LG); the Fondation pour la Recherche Médicale (ECO201806006842 to LG) and Graduate School Life Sciences and Health (to LG). The authors wish to thank the zootechnical platform for animal breeding and care, and genotyping platform at NeuroPSI Saclay.

Appendix A. Supplementary data

Supplementary data to this article can be found online at https://doi.org/10.1016/j.nbd.2023.106163.

References

Albert-gasco, H., Ros-bernal, F., Castillo-Gomez, E., Olucha-Bordonau, F.E., 2020. MAP/ERK signaling in developing cognitive and emotional function and its E ff ect on pathological and neurodegenerative processes. Int. J. Mol. Sci. 21 (4471), 1–30. https://doi.org/10.3390/ijms21124471.

Altafaj, X., Dierssen, M., Baamonde, C., Marti, E., Visa, J., Guimera, J., Oset, M., Gonzalez, J.R., Florez, J., Fillat, C., Estivill, X., 2001. Neurodevelopmental delay, motor abnormalities and cognitive deficits in transgenic mice overexpressing Dyrk1A (minibrain), a murine model of Down's syndrome. Hum. Mol. Genet. 10 (18), 1915–1923. https://doi.org/10.1093/hmg/10.18.1915.

Altman, J., Sudarshan, K., 1975. Postnatal development of locomotion in the laboratory rat. Anim. Behav. 23 (PART 4), 896–920. https://doi.org/10.1016/0003-3472(75)90114-1.

Ammar, M.-R., Humeau, Y., Hanauer, A., Nieswandt, B., Bader, M.-F., Vitale, N., 2013. The Coffin-Lowry syndrome-associated protein RSK2 regulates neurite outgrowth through phosphorylation of phospholipase D1 (PLD1) and synthesis of phosphatidic acid. J. Neurosci.: Off. J. Soc. Neurosci. 33 (50), 19470–19479. https://doi.org/10.1523/JNEUROSCI.2283-13.2013.

Bollen, B., Matrot, B., Ramanantsoa, N., Bergh, O., Van Den Hooge, R.D., Gallego, J., 2012. Olfactory classical conditioning in neonatal mouse pups using thermal stimuli. Behav. Brain Res. 229 (1), 250–256. https://doi.org/10.1016/j.bbr.2011.12.030.

Bruder, J., Fromme, T., 2022. Global adipose tissue remodeling during the first month of postnatal life in mice. Front. Endocrinol. 13 (February), 10–16. https://doi.org/10.3389/fendo.2022.849877.

Castillon, C., Lunion, S., Desvignes, N., Hanauer, A., Laroche, S., Poirier, R., 2018. Selective alteration of adult hippocampal neurogenesis and impaired spatial pattern separation performance in the RSK2-deficient mouse model of Coffin-Lowry syndrome. Neurobiol. Dis. 115 (October 2017), 69–81. https://doi.org/10.1016/j.nbd.2018.04.007.

Chapillon, P., Roullet, P., Lassalle, J.M., 1995. Ontogeny of orientation and spatial learning on the radial maze in mices. Dev. Psychobiol. 28 (8), 429–442. https://doi.org/10.1002/dev.420280805.

Cho, Y.-Y., Yao, K., Bode, A.M., Bergen, H.R., Madden, B.J., Oh, S.M., Ermakova, S., Bong, S.K., Hong, S.C., Shim, J.H., Dong, Z., 2007. RSK2 mediates muscle cell differentiation through regulation of NFAT3. J. Biol. Chem. 282 (11), 8380–8392. https://doi.org/10.1074/jbc.M611322200.

Chuang, N., Mori, S., Yamamoto, A., Jiang, H., Ye, X., Xu, X., Richards, L.J., Nathans, J., Miller, M.I., Toga, A.W., Sidman, R.L., Zhang, J., 2011. An MRI-based atlas and database of the developing mouse brain. NeuroImage 54 (1), 80–89. https://doi.org/10.1016/j.neuroimage.2010.07.043.

Coffin, G.S., 2003. Postmortem findings in the Coffin-Lowry syndrome. Genet. Med. 5 (3), 187–193. https://doi.org/10.1097/01.GIM.0000067991.73943.4F.

Costa, A.P., Lopes, M.W., Rieger, D.K., Barbosa, S.G.R., Gonçalves, F.M., Xikota, J.C., Walz, R., Leal, R.B., 2016. Differential activation of mitogen-activated protein kinases, ERK 1/2, p38MAPKand JNK p54/p46 during postnatal development of rat Hippocampus. Neurochem. Res. 41 (5), 1160–1169. https://doi.org/10.1007/s11064-015-1810-z.

Crawley, J.N., 1999. Behavioral phenotyping of transgenic and knockout mice: experimental design and evaluation of general health, sensory functions, motor abilities, and specific behavioral tests. Brain Res. 835 (1), 18–26. https://doi.org/10.1016/S0006-8993(98)01258-X.

Dierssen, M., Fotaki, V., Martínez de Lagrán, M., Gratacós, M., Arbonés, M.L., Fillat, C., Estivill, X., 2002. Neurobehavioral development of two mouse lines commonly used in transgenic studies. Pharmacol. Biochem. Behav. 73 (1), 19–25. https://doi.org/10.1016/S0091-3057(02)00792-X.

Dufresne, S.D., Bjørbæk, C., El-Haschimi, K., Zhao, Y., Aschenbach, W.G., Moller, D.E., Goodyear, L.J., 2001. Altered extracellular signal-regulated kinase signaling and glycogen metabolism in skeletal muscle from p90 ribosomal S6 kinase 2 knockout mice. Mol. Cell. Biol. 21 (1), 81–87. https://doi.org/10.1128/mcb.21.1.81-87.2001.

Dugani, C.B., Paquin, A., Kaplan, D.R., Miller, F.D., 2010. Coffin-Lowry syndrome: a role for RSK2 in mammalian neurogenesis. Dev. Biol. 347 (2), 348–359. https://doi.org/10.1016/j.ydbio.2010.08.035.

El-haschimi, K., Dufresne, S.D., Hirshman, M.F., Flier, J.S., Goodyear, L.J., Bjørbæk, C., 2003. Insulin Resistance and Lipodystrophy in Mice Lacking Ribosomal S6 Kinase 2, 52(6), pp. 1340–1346. https://doi.org/10.2337/diabetes.52.6.1340.

Eltokhi, A., Kurpiers, B., Pitzer, C., 2020. Behavioral tests assessing neuropsychiatric phenotypes in adolescent mice reveal strain- and sex-specific effects. Sci. Rep. 10 (1), 1–15. https://doi.org/10.1038/s41598-020-67758-0.

Feather-Schussler, D.N., Ferguson, T.S., 2016. A battery of motor tests in a neonatal mouse model of cerebral palsy. J. Vis. Exp. 2016 (117), 1–12. https://doi.org/10.3791/53569.

Fischer, M., Pereira, P.M., Holtmann, B., Simon, C.M., Hanauer, A., Heisenberg, M., Sendtner, M., 2009. P90 ribosomal s6 kinase 2 negatively regulates axon growth in motoneurons. Mol. Cell. Neurosci. 42 (2), 134–141. https://doi.org/10.1016/j.mcn.2009.06.006.

Fischer, M., Cabello, V., Popp, S., Krackow, S., Hommers, L., Deckert, J., Lesch, K.P., Schmitt-Böhrer, A.G., 2017. Rsk2 knockout affects emotional behavior in the IntelliCage. Behav. Genet. 47 (4), 434–448. https://doi.org/10.1007/s10519-017-9853-3.

Fox, W.M., 1965. Reflex-ontogeny and behavioural development of the mouse. Anim. Behav. 13 (2–3), 234–241. https://doi.org/10.1016/0003-3472(65)90041-2.

Gattazzo, F., Laurent, B., Relaix, F., Rouard, H., Didier, N., 2020. Distinct phases of postnatal skeletal muscle growth govern the progressive establishment of muscle stem cell quiescence. Stem Cell Reports 15 (3), 597–611. https://doi.org/10.1016/j.stemcr.2020.07.011.

Haldipur, P., Millen, K.J., 2019. What cerebellar malformations tell us about cerebellar development. Neurosci. Lett. 688 (1), 14–25. https://doi.org/10.1016/j.neulet.2018.05.032.

Henley, J.M., Wilkinson, K.A., 2016. Synaptic AMPA receptor composition in development, plasticity and disease. Nat. Rev. Neurosci. 17 (6), 337–350. https://doi.org/10.1038/nrn.2016.37.

Herrera-Soto, J.A., Santiago-Cornier, A., Segal, L.S., Ramirez, N., Tamai, J., 2007. The musculoskeletal manifestations of the Coffin-Lowry syndrome. J. Pediatr. Orthop. 27 (1), 85–89. https://doi.org/10.1097/01.BPO.0000187994.94515.9D.

Heyser, C.J., 2003. Assessment of developmental milestones in rodents. Curr. Protoc. Neurosci. 25 (1), 1–15. https://doi.org/10.1002/0471142301.ns0818s25.

Hibi, M., Shimizu, T., 2012. Development of the cerebellum and cerebellar neural circuits. Develop. Neurobiol. 72 (3), 282–301. https://doi.org/10.1002/dneu.20875.

Higashi, K., Matsuki, C., 1994. Coffin-Lowry syndrome with sensorineural deafness and labyrinthine anomaly. J. Laryngol. Otol. 108 (2), 147–148. https://doi.org/10.1017/S002221510012612X.

Hirano, T., 2018. Purkinje neurons: development. Morphol. Funct. 699–700 https://doi.org/10.1007/s12311-018-0985-7.

Holtzman, D.M., Santucci, D., Kilbridge, J., Chua-Couzens, J., Fontana, D.J., Daniels, S. E., Johnson, R.M., Chen, K., Sun, Y., Carlson, E., Alleva, E., Epstein, C.J., Mobley, W. C., 1996. Developmental abnormalities and age-related neurodegeneration in a mouse model of down syndrome. Proc. Natl. Acad. Sci. U. S. A. 93 (23), 13333–13338. https://doi.org/10.1073/pnas.93.23.13333.

Hubert, V., Beaunieux, H., Chételat, G., Platel, H., Landeau, B., Danion, J.M., Viader, F., Desgranges, B., Eustache, F., 2007. The dynamic network subserving the three phases of cognitive procedural learning. Hum. Brain Mapp. 28 (12), 1415–1429. https://doi.org/10.1002/hbm.20354.

Hunter, A.G.W., 2002. Coffin-Lowry syndrome: a 20-year follow-up and review of long-term outcomes. Am. J. Med. Genet. 111 (4), 345–355. https://doi.org/10.1002/ajmg.10574.

Jacquot, S., Merienne, K., De Cesare, D., Pannetier, S., Mandel, J.L., Sassone-Corsi, P., Hanauer, A., 1998. Mutation analysis of the RSK2 gene in Coffin-Lowry patients: extensive allelic heterogeneity and a high rate of de novo mutations. Am. J. Hum. Genet. 63 (6), 1631–1640. https://doi.org/10.1086/302153.

Jamon, M., 2014. The development of vestibular system and related functions in mammals: impact of gravity. Front. Integr. Neurosci. 8 (2), 1–13. https://doi.org/10.3389/fnint.2014.00011.

Jero, J., Coling, D.E., Lalwani, A.K., 2001. The use of Preyer's reflex in evaluation of hearing in mice. Acta Otolaryngol. 121 (5), 585–589. https://doi.org/10.1080/000164801316878863.

Jiménez, J.A., Zylka, M.J., 2021. Controlling Litter Effects to Enhance Rigor and Reproducibility With Rodent Models of Neurodevelopmental Disorders, pp. 1–9. https://doi.org/10.1186/s11689-020-09353-y.

Kesler, S.R., Simensen, R.J., Voeller, K., Abidi, F., Stevenson, R.E., Schwartz, C.E., Reiss, A.L., 2007. Altered neurodevelopment associated with mutations of RSK2: a morphometric MRI study of Coffin-Lowry syndrome. Neurogenetics 8 (2), 143–147. https://doi.org/10.1007/s10048-007-0080-6.

Khalaf-Nazzal, R., Francis, F., 2013. Hippocampal development - old and new findings. Neuroscience 248, 225–242. https://doi.org/10.1016/j.neuroscience.2013.05.061.

Lazic, S.E., Essioux, L., 2013. Improving basic and translational science by accounting for litter-to-litter variation in animal models. BMC Neurosci. 14–37 https://doi.org/10.1186/1471-2202-14-37.

Lee, M.H.S., Williams, D.I., 1977. A Longditudinal study of mother-Young interaction in the rat: the effects of infantile stimulation, diurnal rhythms, and pup maturation. Behaviour 63 (3–4), 241–261. https://doi.org/10.1163/156853977X00432.

Llambrich, S., González, R., Albaigès, J., Wouters, J., Marain, F., Himmelreich, U., Sharpe, J., Dierssen, M., Gsell, W., Martínez-Abadías, N., Vande Velde, G., 2022. Multimodal in vivo imaging of the integrated postnatal development of brain and skull and its co-modulation with neurodevelopment in a down syndrome mouse model. Front. Med. 9 (February), 1–16. https://doi.org/10.3389/fmed.2022.815739.

Lo, S.Q., Sng, J.C.G., Augustine, G.J., 2017. Defining a critical period for inhibitory circuits within the somatosensory cortex. Sci. Rep. 7 (1), 1–13. https://doi.org/10.1038/s41598-017-07400-8.

Lopez, C., 2015. Making sense of the body: the role of vestibular signals. Multisens. Res. 28 (5–6), 525–557. https://doi.org/10.1163/22134808-00002490.

Lv, Y., Zhu, L., Zheng, J., Wu, D., Shao, J., 2019. Growth concerns in Coffin–Lowry syndrome: a case report and literature review. Front. Pediatr. 6 (430), 1–5. https://doi.org/10.3389/fped.2018.00430.

Manouvrier-Hanu, S., Amiel, J., Jacquot, S., Merienne, K., Moerman, A., Coëslier, A., Labarriere, F., Vallée, L., Croquette, M.F., Hanauer, A., 1999. Unreported RSK2 missense mutation in two male sibs with an unusually mild form of Coffin-Lowry syndrome. J. Med. Genet. 36 (10), 775–778. https://doi.org/10.1136/jmg.36.10.775.

Marco, E.M., MacRì, S., Laviola, G., 2011. Critical age windows for neurodevelopmental psychiatric disorders: evidence from animal models. Neurotox. Res. 19 (2), 286–307. https://doi.org/10.1007/s12640-010-9205-z.

Marrus, N., Hall, L., 2017. Intellectual disability and language disorder. Child Adolesc. Psychiatr. Clin. N. Am. 26 (3), 539–554. https://doi.org/10.1016/j.chc.2017.03.001.

McRae, J.F., Clayton, S., Fitzgerald, T.W., Kaplanis, J., Prigmore, E., Rajan, D., Sifrim, A., 2017. Prevalence and architecture of de novo mutations in developmental disorders. Nature 542 (7642), 433–438. https://doi.org/10.1038/nature21062.

Mehmood, T., Schneider, A., Sibillec, J., Marques Pereira, P., Pannetier, S., Ammar, M.R., Dembele, D., Thibault-Carpentier, C., Rouach, N., Hanauer, A., 2010. Transcriptome profile reveals AMPA receptor dysfunction in the hippocampus of the Rsk2-knockout mice, an animal model of Coffin-Lowry syndrome. Hum. Genet. https://doi.org/10.1007/s00439-010-0918-0.

Miyata, Y., Saida, K., Kumada, S., Miyake, N., Mashimo, H., Nishida, Y., Shirai, I., Kurihara, E., Nakata, Y., Matsumoto, N., 2018. Periventricular small cystic lesions in a patient with Coffin-Lowry syndrome who exhibited a novel mutation in the RPS6KA3 gene. Brain and Development 40 (7), 566–569. https://doi.org/10.1016/j.braindev.2018.03.012.

Morice, E., Farley, S., Poirier, R., Dallerac, G., Chagneau, C., Pannetier, S., Hanauer, A., Davis, S., Vaillend, C., Laroche, S., 2013. Defective synaptic transmission and structure in the dentate gyrus and selective fear memory impairment in the Rsk2 mutant mouse model of Coffin-Lowry syndrome. Neurobiol. Dis. 58 (10), 156–168. https://doi.org/10.1016/j.nbd.2013.05.016.

Olmos-Serrano, J.L., Tyler, W.A., Cabral, H.J., Haydar, T.F., 2016. Longitudinal measures of cognition in the Ts65Dn mouse: refining windows and defining modalities for therapeutic intervention in down syndrome. Exp. Neurol. 279, 40–56. https://doi.org/10.1016/j.expneurol.2016.02.005.

Pereira, P.M., Schneider, A., Pannetier, S., Heron, D., Hanauer, A., 2010. Coffin-Lowry syndrome. Eur. J. Human Genet.: EJHG 18 (6), 627–633. https://doi.org/10.1038/ejhg.2009.189.

Picker, J.D., Yang, R., Ricceri, L., Berger-Sweeney, J., 2006. An altered neonatal behavioral phenotype in Mecp2 mutant mice. NeuroReport 17 (5), 541–544. https://doi.org/10.1097/01.wnr.0000208995.38695.2f.

Poirier, R., Jacquot, S., Vaillend, C., Soutthiphong, A.A., Libbey, M., Davis, S., Laroche, S., Hanauer, A., Welzl, H., Lipp, H.-P., Wolfer, D.P., 2007. Deletion of the Coffin-Lowry syndrome gene Rsk2 in mice is associated with impaired spatial learning and reduced control of exploratory behavior. Behav. Genet. 37 (1), 31–50. https://doi.org/10.1007/s10519-006-9116-1.

Rauen, K.A., 2013. The RASopathies. Annu. Rev. Genomics Hum. Genet. 14 (1), 355–369. https://doi.org/10.1146/annurev-genom-091212-153523.

Razak, K.A., Dominick, K.C., Erickson, C.A., 2020. Developmental studies in fragile X syndrome. J. Neurodev. Disord. 12 (1), 1–15. https://doi.org/10.1186/s11689-020-09310-9.

Rice, D., Barone, S., 2000. Critical periods of vulnerability for the developing nervous system: evidence from humans and animal models. Environ. Health Perspect. 108 (Suppl. 3), 511–533. https://doi.org/10.1289/ehp.00108s3511.

Santos, M., Silva-Fernandes, A., Oliveira, P., Sousa, N., Maciel, P., 2007. Evidence for abnormal early development in a mouse model of Rett syndrome. Genes Brain Behav. 6 (3), 277–286. https://doi.org/10.1111/j.1601-183X.2006.00258.x.

Schmahmann, J.D., 2019. The cerebellum and cognition. Neurosci. Lett. 688 (April 2018), 62–75. https://doi.org/10.1016/j.neulet.2018.07.005.

Schneider, A., Mehmood, T., Pannetier, S., Hanauer, A., 2011. Altered ERK/MAPK signaling in the hippocampus of the mrsk2_KO mouse model of Coffin-Lowry syndrome. J. Neurochem. 119 (3), 447–459. https://doi.org/10.1111/j.1471-4159.2011.07423.x.

Semple, B.D., Blomgren, K., Gimlin, K., Ferriero, D.M., Noble-Haeusslein, L.J., 2013. Brain development in rodents and humans: identifying benchmarks of maturation and vulnerability to injury across species. Prog. Neurobiol. 106–107 (2013), 1–16. https://doi.org/10.1016/j.pneurobio.2013.04.001.

Shi, D., Xu, S., Waddell, J., Scafidi, S., Roys, S., Gullapalli, R.P., McKenna, M.C., 2012. Longitudinal in vivo developmental changes of metabolites in the hippocampus of Fmr1 knockout mice. Epub 123 (6), 971–981. https://doi.org/10.1111/jnc.12048.

Shi, D., Zhuo, J., Mckenna, C., Gullapalli, P., 2020. White matter alterations in Fmr1 knockout mice during early postnatal. Brain Dev. 21201, 274–289. https://doi.org/10.1159/000506679.

Sudarov, A., Joyner, A.L., 2007. Cerebellum morphogenesis: the foliation pattern is orchestrated by multi-cellular anchoring centers. Neural Dev. 2 (1) https://doi.org/10.1186/1749-8104-2-26.

Sun, Y., Liu, W., Liu, T., Feng, X., Yang, N., Zhou, H., 2016. Signaling Pathway of MAPK/ERK in Cell Proliferation, Differentiation, Migration, Senescence and Apoptosis, 9893(October). https://doi.org/10.3109/10799893.2015.1030412.

Toso, L., Cameroni, I., Roberson, R., Abebe, D., Bissell, S., Spong, C.Y., 2008. Prevention of developmental delays in a down syndrome mouse model. Obstet. Gynecol. 112 (6), 1242–1251. https://doi.org/10.1097/AOG.0b013e31818c91dc.

Trivier, E., De Cesare, D., Jacquot, S., Pannetier, S., Zackai, E., Young, I., Mandel, J.L., Sassone-Corsi, P., Hanauer, A., 1996. Mutations in the kinase Rsk-2 associated with Coffin-Lowry syndrome. Nature 384 (6609), 567–570. https://doi.org/10.1038/384567a0.

Vissers, L.E.L.M., Gilissen, C., Veltman, J.A., 2015. Genetic studies in intellectual disability and related disorders. Nat. Rev. Genet. 17 (1), 9–18. https://doi.org/10.1038/nrg3999.

Weber, E.M., Olsson, I.A.S., 2008. Maternal behaviour in Mus musculus sp.: an ethological review. Appl. Anim. Behav. Sci. 114 (1–2), 1–22. https://doi.org/10.1016/j.applanim.2008.06.006.

Wood, S.L., Beyer, B.K., Cappon, G.D., 2003. Species comparison of postnatal CNS development: functional measures. Birth Def. Res. Part B - Develop. Reprod. Toxicol. 68 (5), 391–407. https://doi.org/10.1002/bdrb.10037.

Yang, X., Matsuda, K., Bialek, P., Jacquot, S., Masuoka, H.C., Schinke, T., Li, L., Brancorsini, S., Sassone-Corsi, P., Townes, T.M., Hanauer, A., Karsenty, G., 2004. ATF4 is a substrate of RSK2 and an essential regulator of osteoblast biology; implication for Coffin-Lowry syndrome. Cell 117 (3), 387–398. https://doi.org/10.1016/s0092-8674(04)00344-7.

Yoo, H., Mihaila, D.M., 2022. Rooting Reflex. Definitions, pp. 2–5 (Booksheld ID: NBK557636).